Local Density Approximation for Excited States

Tim Gould[*]

Queensland Micro- and Nanotechnology Centre, Griffith University, Nathan, Qld 4111, Australia

Stefano Pittalis

CNR-Istituto Nanoscienze, Via Campi 213A, I-41125 Modena, Italy

The ground state of an homogeneous electron gas is a paradigmatic state that has been used to model and predict the electronic structure of matter at equilibrium for nearly a century. For half a century, it has been successfully used to predict ground states of quantum systems via the local density approximation (LDA) of density functional theory (DFT), and systematic improvements in the form of generalized gradient approximations and evolution thereon. Here, we introduce the LDA for excited states by considering a particular class of nonthermal ensemble states of the homogeneous electron gas. These states find sound foundation and application in ensemble DFT—a generalization of DFT that can deal with ground and excited states on equal footing. The ensemble LDA is shown to successfully predict difficult low-lying excitations in atoms and molecules for which approximations based on local spin density approximation and time-dependent LDA fail.

I. INTRODUCTION

Excitation of many-electron systems characterizes novel states of matter and increasingly permeates the functions of novel advanced technologies. In problems ranging from photovoltaic devices to quantum dots, nanoparticle catalysts, and quantum computing devices, particlelike, collective, or topological excitations are exploited coherently. Challenges are multidisciplinary, yet solutions can be inspired—and, increasingly, predicted—by computationally investigating quantum structures and mechanisms at the nanoscale. Density functional theory (DFT) [1,2] has dominated the stage of computational electronic structure methodologies since the 1960s by balancing accuracy with efficiency. But DFT does not handle excited states directly, being restricted to addressing eigenstates of lowest energy (i.e., ground states). This work will show how successful DFT methods for ground states can be upgraded into methods for also tackling excited states.

The most fundamental model from which DFT gained inspiration can be traced back to the seminal works by Thomas [3] and Fermi [4]. In 1927, they independently proposed a remarkable approximation for quantum physics—that the state of any many-electron system can be modeled by referring, via the particle density (a local quantity), to a homogeneous gas (HEG) of electrons. Because of its poor treatment of kinetic energy contributions, the resulting Thomas-Fermi approximation (TFA) is not very good in practice. But almost all modern modeling of electronic structure employs its spiritual descendent, in the form of Kohn-Sham (KS) DFT [1,2]: (1) kinetic energy contributions are treated quantum mechanically, via a noninteracting auxilliary system, (2) the energy of electrostatic interactions is treated clasically, for any given particle density, and (3) the HEG is only used to treat the remaining quantum exchange-correlation (xc) energy contributions.

The HEG [5] is, arguably, the simplest many-electron system. It involves $N \to \infty$ electrons interacting in response to a uniform positive background charge of fixed density n and volume $V = N/n \to \infty$. The resulting (interacting) electronic structure problem can be solved semianalytically in its high-density and low-density limits, and to high accuracy for moderate densities using quantum Monte Carlo (QMC) techniques [6–8]. The *known* paradigmatic xc behavior of HEG may then be used to approximate the *unknown* xc behavior of inhomogeneous quantum systems, via parametrizations [9–11]. Crucially, it has also been recognized that the local density approximation (LDA) provides exact leading terms in a semiclassical expansion of any quantum system, under appropriate limits [12–16],

---

[*]Contact author: t.gould@griffith.edu.au

which helps to explain the ongoing success of the Jacob's ladder [17] philosophy of systematically improving on the LDA [18–21].

What about excited states? In the late 1980s, the time-dependent extension of DFT (TDDFT) was revealed to be a highly effective tool for simulating spectra, via a perturbative (linear-response) expansion around the ground state. But, despite its ongoing success, it was soon revealed [22,23] that approximations to TDDFT could not describe important double excitations at all, and struggled to describe charge transfer excitations except by using specialized approximations [24–26]. More recently, singlet-triplet inversion [27] (with great promise for photovoltaics) has emerged as another important problem where TDDFT struggles [28,29].

In parallel with TDDFT, Kohn and collaborators put forward a density functional theory for *stationary* excitations based on mixed states (ensembles) rather than pure states: ensemble DFT (EDFT) [30,31]. Unlike the perturbation-based formalism of TDDFT, EDFT recast the problem of computing excited states into an extended "ground-state-like" problem involving variational minima. TDDFT's rapid success in predicting spectra, and challenges in constructing useful ensemble approximations, initially led to EDFT falling by the wayside. Recently, however, it has reemerged as a powerful alternative to TDDFT because approximations in EDFT can solve precisely those excitation problems for which TDDFT struggles or fails [32–45].

Moreover, recent theoretical breakthroughs [37,46–50] have revealed aspects of the architecture of key functional forms in EDFT that have opened unprecedented possibilities for novel approximations for excited states. The change of perspective brought about by EDFT compared to (TD)DFT is radical: (1) the auxiliary states of the Kohn-Sham ensemble can acquire the form of coherent (finite) superposition of Slater determinants (rather than the "disentangled" single determinant for pure ground states), (2) the ensemble Hartree energy (in contrast to the *classical* Hartree energy) accounts for peculiar quantum features, (3) the ensemble exchange energy does not (necessarily) reduce to textbook Fock-exchange expressions, and (4) in addition to regular looking state-driven (SD) correlations, unusual density-driven (DD) correlations emerge.

In this work, we demonstrate that the same system of knowledge allows us to derive an exchange-correlation energy approximation from first principles (*ab initio*). We consider the prominent example of approximations that are derivable from the HEG. Given nearly 100 years of exploration, one might expect the HEG to have given up all its useful secrets. Crucially this work reveals that when the HEG is viewed from the perspective of EDFT, we can introduce a class of nonthermal ensembles from which we can derive a local approximation for excited states *directly*. The regular LDA has provided a highly effective

cornerstone for systematic improvements for ground states—both as the first rung of Jacob's ladder [17] and as a paradigmatic limit that can constrain functional forms [18–20,51]. The ensemble LDA developed in this work therefore provides us with a (long-sought) cornerstone for systematic improvements to approximations for excited states.

The remainder of this work is organized as follows. Section II gives an introduction to the HEG in the context of density functional theory and briefly reviews relevant attempts that predate our current proposal. Section III introduces the elements of ensemble DFT which are exploited in the novel parts of the work and presents the relevant ensemble states of HEG, which are designed to capture excited-state physics in crucial energy components of the HEG ensemble states (Appendix D reports a parametrization). Sections IV and V demonstrate the practical usefulness of the formal developments done by setting up (Sec. IV) and applying (Sec. V) an ensemble LDA to atoms and molecules. Finally, Sec. VI summarizes the work, looks toward the near future, and draws conclusions.

II. LOCAL DENSITY APPROXIMATION

This section will first motivate the standard approach to understanding HEGs, in the context of density functional theory, to lay out the foundation of the LDA. Section III then introduces ensemble density functional theory and excited state HEGs as the foundations of the excited-state LDA (eLDA). Together, these sections provide the key theoretical tools for the rest of the work. Throughout, we use atomic units so that lengths are expressed in Bohr and energies are expressed in Hartree.

Before getting to the details, it is worth noting that the properties of HEGs are conventionally defined using the Wigner-Seitz radius, $r_s := (3/4\pi n)^{1/3} \approx 0.620350 n^{-1/3}$, and spin-polarization factor, $\zeta = (n_\uparrow - n_\downarrow/n)$. Here, n is the density of electrons and $n_{\uparrow,\downarrow}$ are the densities of $\uparrow, \downarrow$ electrons obeying $n_\uparrow + n_\downarrow = n$. This combination of terms reflects the fact that interactions between same- and different-spin electrons are fundamentally different due to the Pauli exclusion principle, so energies change not only with the total density but also the relative contributions of majority ($\uparrow$) and minority ($\downarrow$) electrons to the density. We will sometimes use n instead of r_s to clarify dependence on the density.

A. DFT of homogeneous electron gases

DFT provides an important tool for the analysis and parametrization of HEGs. Key theorems [1,52,53] demonstrate that all properties of a quantum mechanical ground state are described by its density $n(r)$ (constant, n in an HEG). This is easily extended to spin DFT [54], which covers *de facto* ground states like the lowest energy with a given spin polarization $\zeta(r)$ (constant ζ in an HEG). DFT is

typically used synonymously with KS DFT, [2] and we shall adopt this convention throughout.

In Kohn-Sham DFT, the ground state energy of an N-electron system in external (nuclear) potential $v(\boldsymbol{r})$ is written as

$$E_0[n] := T_s[n] + \int nv d\boldsymbol{r} + E_{\mathrm{H}}[n] + E_{\mathrm{x}}[n] + E_{\mathrm{c}}[n], \quad (1)$$

where $[n]$ indicates a functional of the density $n(\boldsymbol{r})$, obeying $\int n d\boldsymbol{r} = N$. Useful exact energy expressions are known for [55]

(1) the Kohn-Sham kinetic energy functional $T_s[n]$ that includes kinetic energy effects from a *noninteracting* system with the same density (and spin)—we may write $T_s = \sum_{i\sigma \in \mathrm{occ}} \int \frac{1}{2} |\nabla \phi_{i\sigma}(\boldsymbol{r})|^2 d\boldsymbol{r}$ using a set of occupied Kohn-Sham orbitals $\phi_{i\sigma}(\boldsymbol{r})$ [2],
(2) the Hartree energy functional, $E_{\mathrm{H}}[n] = U[n]$, that includes mean-field electrostatic interactions,
(3) the Fock exchange energy functional, $E_{\mathrm{x}}[n] = -\sum_{ii'\sigma \in \mathrm{occ}} U[\phi_{i\sigma}\phi_{i'\sigma}^*]$, that includes corrections for fermionic exchange based on the same non-interacting system used for T_s.

The *unknown* correlation energy functional $E_{\mathrm{c}}[n]$ captures classical and quantum contributions that are missed in the other terms.

Here we introduced an electrostatic Coulomb integral,

$$U[\rho] = \int \rho(\boldsymbol{r})\rho^*(\boldsymbol{r}') \frac{d\boldsymbol{r} d\boldsymbol{r}'}{2|\boldsymbol{r}-\boldsymbol{r}'|} = U[\rho^*] \quad (2)$$

that was adapted for complex-valued inputs to accommodate classical (here, in E_{H} only) and quantum (here, in E_{x} only) interactions. All functionals are readily extended to spin-polarized ground states by introducing the number, $N_\uparrow \le N$, of $\uparrow$ electrons ($N_\downarrow = N - N_\uparrow$) as an additional constraint, or equivalently setting $\zeta = (N_\uparrow - N_\downarrow)/N$. Precise details do not matter at this point and will be introduced as required.

In a standard HEG, the mean-field Hartree contribution (from E_{H}) is canceled exactly by the positive background charge. The energy per particle, $e = E/N$, of an HEG may therefore be separated into three components,

$$e(n,\zeta) = t_s(n,\zeta) + \epsilon_{\mathrm{x}}(n,\zeta) + \epsilon_{\mathrm{c}}(n,\zeta), \quad (3)$$

using Eq. (1). Here, n and ζ are scalar constants, and $t_s := T_s/N$, $\epsilon_{\mathrm{x}} := E_{\mathrm{x}}/N$, and $\epsilon_{\mathrm{c}} := E_{\mathrm{c}}/N$ are energy densities per particle. The Kohn-Sham kinetic and exchange energies may be obtained analytically, and are

$$t_s(r_s,\zeta) = t_s(r_s)\frac{(1+\zeta)^{5/3} + (1-\zeta)^{5/3}}{2}$$
$$:= t_s(r_s)f_s(\zeta), \quad (4)$$

$$\epsilon_{\mathrm{x}}(r_s,\zeta) = \epsilon_{\mathrm{x}}(r_s)\frac{(1+\zeta)^{4/3} + (1-\zeta)^{4/3}}{2}$$
$$:= \epsilon_{\mathrm{x}}(r_s)f_{\mathrm{x}}(\zeta), \quad (5)$$

where

$$t_s(r_s) := \frac{C_t}{r_s^2} = \frac{3}{10}\left(\frac{9\pi}{4}\right)^{2/3}r_s^{-2} = 1.10495 r_s^{-2}, \quad (6)$$

$$\epsilon_{\mathrm{x}}(r_s) := \frac{-C_x}{r_s} = -\frac{3}{4\pi}\left(\frac{9\pi}{4}\right)^{1/3}r_s^{-1} = -0.458165 r_s^{-1} \quad (7)$$

are the kinetic and exchange energies of an unpolarized HEG (in atomic units). We may alternately write $t_s(n) = 2.87123 n^{2/3}$ and $\epsilon_{\mathrm{x}}(n) = -0.738559 n^{1/3}$.

The final ingredient is the correlation energy term,

$$\epsilon_{\mathrm{c}}(r_s,\zeta) := \sum_k \epsilon_{\mathrm{c}}^k(r_s)f_{\mathrm{c}}^k(\zeta), \quad (8)$$

which has known series expansions for the high- ($r_s \to 0$) and low-density ($r_s \to \infty$) limits, but is unknown in general. Total energies e^{QMC} of HEGs may be evaluated to high accuracy via quantum Monte Carlo simulations, which have served to supplement limiting cases since the pioneering work by Ceperley and Alder [6]. Then, $\epsilon_{\mathrm{c}} = e^{\mathrm{QMC}} - t_s - \epsilon_{\mathrm{x}}$ may be parametrized (see, e.g., Refs. [9–11]) by a truncated series in the general form of Eq. (8). Models and parameters for ϵ_{c} are usually designed to satisfy or approximately satisfy limiting behaviors of HEGs, with some free parameters that can be optimized to reproduce reference data from QMC at intermediate values.

B. From HEGs to real systems

The LDA models the quantum mechanics of an inhomogeneous system by combining exact DFT terms with terms reusing expressions from HEGs. In detail, for an inhomogeneous system with nuclear potential v and electronic density n, the LDA yields a ground state energy:

$$E_{\mathrm{LDA}}[n] = T_s[n] + \int nv d\boldsymbol{r} + E_{\mathrm{H}}[n] + \int n\epsilon_{\mathrm{xc}} d\boldsymbol{r}. \quad (9)$$

The first three terms of Eq. (9) have the same form as the corresponding exact terms. HEGs are used to approximate the xc energy, $E_{\mathrm{xc}}[n] \approx E_{\mathrm{x}}^{\mathrm{LDA}}[n] + E_{\mathrm{c}}^{\mathrm{LDA}}[n]$. Specifically, the xc energy density is locally approximated by using the xc energy per unit particle, $\epsilon_{\mathrm{xc}}(\boldsymbol{r}) = \epsilon_{\mathrm{x}}(n(\boldsymbol{r})) + \epsilon_{\mathrm{c}}(n(\boldsymbol{r}))$ [from Eqs. (7) and (8)], of an HEG with density $n(\boldsymbol{r})$.

The LDA is an important component of many successful density functional approximations (DFAs) and is the cornerstone of "Jacob's ladder" [17] for DFAs. Its success is typically justified by arguments based on "xc holes" that also help in extending LDAs to incorporate *semilocal*

properties like density gradients or metadensities [56]. Successes of the TFA—which also approximates the non-interacting kinetic energy by an LDA—and of the usual KS LDA have also been justified by appealing to exact semi-classical limits and universal bounds for quantum mechanical systems [12–16,57]. It should not be forgotten, however, that without the initial judicious choice by Kohn and Sham of *not* changing the form of T_s and E_H, the broad success of DFT would not have gone much beyond the much more limited success of the TFA.

One of the most important and earliest extensions of the LDA is the local *spin* density approximation (LSDA) [58], which uses the local densities, $n_\uparrow(r)$ and $n_\downarrow(r)$, of the two spin channels separately. Equation (9) is extended to $E_{LSDA}[n_\uparrow, n_\downarrow] = T_s[n_\uparrow, n_\downarrow] + \int nv dr + E_H[n] + \int n\epsilon_{xc}(n, \zeta) dr$, which includes the effect of spin in T_s by allowing the orbitals to differ for different spin channel and uses the local density, $n(r) = n_\uparrow(r) + n_\downarrow(r)$, and spin polarization, $\zeta(r) = [n_\uparrow(r) - n_\downarrow(r)]/N$, in the HEG parametrization. The LDA then becomes the special case $n_\uparrow = n_\downarrow$. Indeed the LSDA is the true cornerstone of almost all modern DFT applications because, by introducing spin, it extends the applicability of HEG-based approximations to spin-polarized states; i.e., either ground states acted upon a (collinear) magnetic field, or the lowest excited state of a given net spin-polarization. A natural next step would be to extend the LDA to stationary but otherwise general *excited* states.

C. Long-standing conundrum: Local approximations for excitations

Let us begin by highlighting why the eLDA problem is more difficult than ground states. Firstly, DFT itself is not well defined for excited states, so one needs to work out what terms should be treated exactly, or by approximations, or other extensions [59,60]. Secondly, the spectra of molecules is discrete and the spectra of insulators is gapped, whereas HEGs are a metal with no gap and a continuous (dense) spectrum; the eLDA must therefore map between fundamentally different physics. Finally, excitations innately invoke nonlocal physics (e.g., via the underlying *global* reciprocal orthogonality conditions for the corresponding eigenstates, or the transfer of electrons through a subset of orbitals in transitions) which challenges the use of only local properties like the particle and spin-polarization densities. Despite these fundamental difficulties, various attempts have been made to produce eLDAs, as surveyed below.

An early attempt was by Kohn [61], who sought to connect inhomogeneous excited states with finite temperature HEGs by enforcing a relation between auxiliary ensembles of excited states and proper thermal ensembles. Kohn's approach implies to deal with quantities like the entropy, heat capacity, and temperature, thus reducing the problem of finding excitation energies to the problem of finding some key aspect of the thermodynamics of a

system. Because the approach involves an effective temperature to be estimated by integrating entropies per unit volume over the *whole* space [see Eq. (26) in Ref. [62] for a helpful discussion], Kohn does not regard the approach as a purely local density approximation but defines it to be a *quasi-LDA*. This approximation was used in a foundational paper on excited state EDFT [62], but its restriction to averages over multiple excited states meant that it could not resolve singlet-triplet spin splitting.

Theophilou and Papaconstantinou [63] later introduced an eLDA in which the reference to thermodynamics was finally removed. They also added the important spin dependence, useful to evaluate spin splittings. Their approach reduces to the LSDA in which the spin polarization is replaced with a global quantity (independent of space) that is related to the spin state of the underlying spin-restricted symmetry adapted approach, and is therefore a quasi-LSDA.

Harbola and co-workers [64,65] were able to exploit the exchange energy of *proper* excited HEGs to derive an LDA thereto. Their approach is most similar in spirit to the work presented here. However, their approach does not go beyond exchange, possibly because they used the conventional ground state DFT framework instead of EDFT. Furthermore, orbital-dependent self-interaction-correction terms must be included as well.

A much more recent attempt, that works within the framework of EDFT, is from Loos and co-workers [41,42] who parametrized a local density approximation for ensembles based on the properties of uniform electron gases with finite numbers of electrons [66–69]. Their approach captures important excited-state physics, notably by avoiding the issue of a continuous spectra in the HEG, and is explicitly designed for EDFT problems. However, applications were presented only for two-electron systems, and extensions are required to make the approach more generally applicable.

Finally, "combination rules" have recently been identified that allow reuse of *any* existing ground state DFA, including L(S)DA, for use in excited-state problems [44,45]. Therefore, combination rules highlight that the locality assumptions behind LDAs can be extended to excited states. This is because combination rules are equivalent to setting (for a specific excited state) $n\epsilon_{xc}^{excited}(n) \approx \sum_P c_P n_P \epsilon_{xc}^{DFA}(n_P)$ in $E_{xc}^{excited} = \int n\epsilon_{xc}^{excited} dr$, where P labels auxiliary states, n_P are their densities, c_P are constants, and ϵ_{xc}^{DFA} is an existing (semi)local DFA. It follows that the locality of ϵ_{xc}^{DFA} is extended through the weighted sum in $\epsilon_{xc}^{excited}$. Despite being exact for exchange and working effectively for xc DFAs [44], the rules are *inexact* for correlations, meaning there is room for improvement. The approach presented here may thus be regarded as a first step toward circumventing combination rules, by replacing them with an excited-state LDA foundation.

Crucially, we should stress that previous attempts (except the combination rules) were made by working

with an *incomplete* understanding of the structure of the relevant exact density functionals for excited states. In particular, recent analysis has revealed that Hartree and exchange in EDFT go beyond the previous restrictive— sometimes even problematic—definitions [46,49]. We now know that correlations come in two kinds: state driven (which resemble ground state correlations) and density driven (which are totally new). All new terms in the ensemble Hartree and DD correlation are highly nonlocal expressions. Recent progress has also revealed that regular DFT approximations (and thus LDA expressions) are appropriate for the novel exchange terms and the novel SD-correlation terms [44,49]—more below. Thus, in Sec. III, we show that the aforementioned novel components can be determined *also* in HEGs.

III. EDFT OF EXCITED-STATE HEGS

As discussed in Sec. II C, previous attempts to develop excited-state LDAs have run into problems or limitations. It is reasonable to assume that some of these difficulties reflect the fact that previous work was based on incomplete understanding of the structure of excited states. This section thus first (Sec. III A) discusses an upgraded and first principles understanding of how the excited-states physics can be encoded into the relevant energy components of EDFT. From these foundations it becomes easier to discern which HEG expressions may be used to approximate which exact energy component in inhomogeneous systems, as a first enabling step toward an effective excited-state LDA.

Section III B then introduces and derives a "constant occupation factor ensemble" (cofe) HEG to serve as a foundation for excited-state approximations. The results derived in this section are later applied to inhomogeneous systems in Sec. IV, which also expands on why and how the cofe HEG is relevant. Results on realistic systems are then presented in Sec. V.

A. Ensemble DFT from first principles

To understand ensemble DFT [30,31], let us first define quantum state ensembles. A (quantum state) ensemble $\hat{\Gamma}$ is an operator that describes a classical mixture of quantum states. It may be defined using a spectral representation,

$$\hat{\Gamma} = \sum_\kappa w_\kappa |\kappa\rangle\langle\kappa|, \qquad 0 \leq w_\kappa \leq 1, \qquad \sum_\kappa w_\kappa = 1, \quad (10)$$

in which an arbitrary set of orthonormal quantum states $|\kappa\rangle$ are assigned probabilities or weights w_κ. Operator expectation values, $\bar{O} = \langle\Psi|\hat{O}|\Psi\rangle$, are replaced by $\bar{O}^w = \mathrm{Tr}[\hat{\Gamma}^w \hat{O}] = \sum_\kappa w_\kappa \langle\kappa|\hat{O}|\kappa\rangle$, which involves quantum and classical averages. Ensembles are more flexible than wave functions, so can describe constrained, open, and degenerate systems that are otherwise outside the remit of wave function mechanics or DFT. Various theorems [30,31,70] extend key results

of DFT to ensembles, including important variational principles.

In excited-state EDFT, the usual variational formula, $E_0 = \min_\Psi \langle\Psi|\hat{H}|\Psi\rangle$, is replaced by the weighted average,

$$E^w := \inf_{\hat{\Gamma}^w} \mathrm{Tr}[\hat{\Gamma}^w \hat{H}] = \sum_\kappa w_\kappa E_\kappa, \qquad (11)$$

where $\hat{\Gamma}^w$ is an ensemble with a given set of weights $w = \{w_0, w_1, \ldots\}$, and E_κ are eigenenergies of $\hat{H}$ ordered such that the lowest energies are associated with the largest weights. The energies are in usual ascending "excitation" order if we define the weights to be monotonically decreasing, i.e., $w_{\kappa'} \leq w_\kappa$ for $E_{\kappa'} \geq E_\kappa$. Note that we follow the usual convention of using superscripts w (or cofe later) to identify ensemble functionals. But we depart from the recent convention of using calligraphic letters to avoid confusion between $\mathcal{E}$ for total energies of ensembles and ϵ for energies per particle of HEGs.

It is convenient to generalize Eq. (1) to ensembles by writing

$$E^w[n] := T_s^w[n] + \int nv\, d\mathbf{r} + E_\mathrm{H}^w[n] + E_\mathrm{x}^w[n] + E_\mathrm{c}^w[n]. \qquad (12)$$

Here, w indicates the set of weights, n is the density, and v is the external potential. In a Kohn-Sham formalism, the ensemble density is conveniently written as

$$n^w(\mathbf{r}) := \sum_i f_i^w n_i(\mathbf{r}), \qquad f_i^w := \sum_\kappa w_\kappa \theta_i^\kappa, \qquad (13)$$

in terms of orbital densities, $n_i(\mathbf{r}) := |\phi_i(\mathbf{r})|^2$, and average occupation factors f_i^w, which may be noninteger and involve a weighted average over the integer occupation factors, $\theta_i^\kappa \in (0, 1, 2)$ (i.e., no occupation, occupation in one spin, or occupation in both spins) of each KS state in the ensemble. The orbitals obey a spin-independent KS-like equation, $[\hat{t} + v_s^w(\mathbf{r})]\phi_i(\mathbf{r}) = \varepsilon_i\phi_i(\mathbf{r})$, where $\hat{t} \equiv -\frac{1}{2}\nabla^2$ is the one-body kinetic energy operator. Note, functions of the position like orbitals ($\phi_i \equiv \phi_i^w$) and densities ($n_i \equiv |\phi_i^w|^2$ and similar) also carry an *implicit* dependence on the weights w as do KS wave functions ($|\kappa_s\rangle \equiv |\kappa_s^w\rangle$), but we leave the superscript off to avoid clutter in equations.

With the ensemble formalism defined, we are now ready to define the terms in Eq. (12). Recent work [46,47,49] has sought to rigorously define exact energy functionals for excited-state ensembles, giving

$$T_s^w[n] := \sum_i f_i^w \int \frac{1}{2}|\nabla\phi_i|^2 d\mathbf{r}, \qquad (14)$$

$$E_\mathrm{H}^w[n] := \sum_{\kappa\kappa'} w_{\max(\kappa,\kappa')} U[n_{s,\kappa\kappa'}], \qquad (15)$$

$$E_x^w[n] := -\sum_{ii'} f_{\max(i,i')}^w U[\phi_i \phi_{i'}^*]. \tag{16}$$

Here, we used $\int \phi^* \hat{t} \phi d\mathbf{r} = \int \frac{1}{2} |\nabla \phi|^2 d\mathbf{r}$, $U[\rho]$ as defined earlier in Eq. (2), introduced $n_{s,\kappa\kappa}(\mathbf{r}) = \langle \kappa_s | \hat{n}(\mathbf{r}) | \kappa_s \rangle$ as the density of Kohn-Sham state $|\kappa_s\rangle$, and introduced $n_{s,\kappa\neq\kappa'}(\mathbf{r}) = \langle \kappa_s | \hat{n}(\mathbf{r}) | \kappa_s' \rangle$ as the (potentially complex-valued) transition density between Kohn-Sham states $|\kappa_s\rangle$ and $|\kappa_s'\rangle$. Equation (14) retains its well-known "textbook" expression in all cases. By contrast, Eqs. (15) and (16) *reproduce* textbook expressions for the lowest energy state of each spin-polarization (maximal $|S_z|$) only—i.e., "conventional" states accessible by ground state DFT—but are different in ensembles and excited states.

The remaining energy, $E_c^w := E^w - \int nv d\mathbf{r} - T_s^w - E_H^w - E_x^w$, is the unknown correlation energy functional. It is convenient to partition

$$E_c^w[n] := E_c^{SD,w}[n] + E_c^{DD,w}[n] \tag{17}$$

into state-driven and density-driven components, each with different physical origins [47–49]. The SD correlation energy may be written as

$$E_c^{SD,w} := \int_0^1 d\lambda \int_0^\infty \frac{-d\omega}{\pi} \int \frac{d\mathbf{r}d\mathbf{r}'}{2|\mathbf{r}-\mathbf{r}'|}$$
$$\times [\chi_\lambda^w(\mathbf{r},\mathbf{r}';i\omega) - \chi_0^w(\mathbf{r},\mathbf{r}';i\omega)], \tag{18}$$

in terms of density-density response function [see Ref. [49] for details], and retains the same general expression as the ground state correlation energy. The density-driven term is always zero in conventional states (e.g., molecular ground states) so is not considered in ground state DFT. We shall address its general expression shortly.

It is sometimes useful to rewrite Eqs. (15) and (16) as

$$E_{H/x}^w = \int n_{2,H/x}^w(\mathbf{r},\mathbf{r}') \frac{d\mathbf{r}d\mathbf{r}'}{2|\mathbf{r}-\mathbf{r}'|} \tag{19}$$

using the ensemble Hartree and exchange pair densities,

$$n_{2,H}^w(\mathbf{r},\mathbf{r}') = \sum_{\kappa\kappa'} w_{\max(\kappa,\kappa')} n_{s,\kappa\kappa'}(\mathbf{r}) n_{s,\kappa'\kappa}(\mathbf{r}'), \tag{20}$$

$$n_{2,x}^w(\mathbf{r},\mathbf{r}') = -\sum_{ii'} f_{\max(i,i')} \rho_i(\mathbf{r},\mathbf{r}') \rho_{i'}^*(\mathbf{r},\mathbf{r}'), \tag{21}$$

where $\rho_i(\mathbf{r},\mathbf{r}') = \phi_i(\mathbf{r})\phi_i^*(\mathbf{r}')$. It is straightforward to see that using Eqs. (20) and (21) in Eq. (19) gives the same energies as Eqs. (15) and (16), respectively. The DD correlation energy also can be expressed using Eq. (19). Its pair density has a similar form to the Hartree energy,

$$n_{2,c}^{DD,w}(\mathbf{r},\mathbf{r}') = \sum_{\kappa\kappa'} w_{\max(\kappa,\kappa')} \int_0^1 [n_{\kappa\kappa'}^\lambda(\mathbf{r}) n_{\kappa'\kappa}^\lambda(\mathbf{r}')$$
$$- n_{s,\kappa\kappa'}(\mathbf{r}) n_{s,\kappa'\kappa}(\mathbf{r}')] d\lambda, \tag{22}$$

but involves the difference between transition densities at interaction strength λ and their KS counterparts (i.e., $\lambda = 0$) [49]. Thus, like the Hartree energy, $E_c^{DD,w}$ has an explicitly nonlocal dependence on densities and orbitals and should not by approximated locally. Details and other helpful relationships for functionals will be introduced and used as required.

Before proceeding further, we make the important assumption that the results of Sec. III A apply to HEGs. This is an assumption because all EDFT results shown so far are for *finite* systems with *countable* numbers of excitations. By contrast, homogeneous electron gases are *infinite* and their excitations are *uncountable*. The rest of this paper treats HEGs as the appropriate thermodynamic limit of finite systems whose properties are consistent with the ensemble density functional theory presented in this section, and so obey straightforward generalizations of key equations.

B. cofe HEGs

With core theory now established, let us proceed to explore generalizations of HEG physics that exploit the additional degrees of freedom from ensembles. Our aim is to develop an understanding of HEGs that spans ground state and excited-state physics. To that end, we will reveal the properties of constant occupation factor ensemble HEGs—the meaning of the name will soon become apparent. The key to generalizations is to invoke both ground and excited states of HEGs. As we shall show below, many properties are then uniquely determined by the occupation factors f_q of the HEG, while others depend on w explicitly, so require some extra restrictions on the nature of excited states because there can be many different sets of weights w that yield a given f_q.

Equations (13), (14), and (16) reveal that the density, kinetic energy, and exchange energy of any ensemble system depend explicitly only on the orbital occupation factors f_i^w. In HEGs, we replace f_i^w by f_q, i.e., as a function of absolute wave number q. This follows from the fact that (i) the KS "orbitals" of an HEG are plane waves $\phi_q(\mathbf{r}) \propto e^{i\mathbf{q}\cdot\mathbf{r}}$ and (ii) that KS minimization dictates that we fill each $q = |\mathbf{q}|$ in full. Thus, given f_q it is possible to define the density n as well as the kinetic and exchange energies. We will therefore first discuss some HEGs from the perspective of orbital occupation factors, before proceeding to refine the definition.

The most intuitive form of HEG is an unpolarized gas in the lowest energy (ground) state. In orbital (KS) terms, the unpolarized HEG noninteracting ground state is a Slater determinant of doubly occupied plane-wave orbitals.

Occupied states fill in $\uparrow/\downarrow$ pairs up to a single Fermi wave number k_F. Its wave-number-dependent occupation factor and density are

$$f_q^{\text{unpol}} = 2\Theta(k_F - q), \qquad k_F = (3\pi^2 n)^{1/3}, \quad (23)$$

where $\Theta(x) = \{1 \;\; \forall \, x \geq 0; 0 \;\; \forall \, x < 0\}$ is a Heaviside step function. The density n of the gas is sufficient to describe the state.

Ground states realized by exposing the HEG to a uniform external magnetic field (the corresponding vector potential being ignored, as in spin DFT) have a wave-number-dependent occupation factor determined by spin-dependent Fermi wave numbers:

$$f_q^{\text{pol}} = \Theta(k_F^{\uparrow} - q) + \Theta(k_F^{\downarrow} - q), \quad k_F^{\uparrow,\downarrow} = (6\pi^2 n_{\uparrow,\downarrow})^{1/3}. \quad (24)$$

The unpolarized gas is then the special case of $n_{\uparrow} = n_{\downarrow} = (n/2)$ giving $\zeta = 0$. A fully polarized gas has $n_{\uparrow} = n$, $n_{\downarrow} = 0$, and $\zeta = 1$. For definiteness, we work under the convention that the majority spin channel is the "up" ($\uparrow$) channel. The density n and spin polarization ζ are sufficient to describe the state.

In this work, we consider (nonthermal) *ensembles* of excited states, which correspond to *averaged* occupation factors. Specifically, we consider ensembles obeying

$$f_q^{\text{cofe}} = \bar{f}\Theta(\bar{k}_F^{\text{cofe}} - q), \qquad \bar{k}_F^{\text{cofe}} = (6\pi^2 n/\bar{f})^{1/3}. \quad (25)$$

The bar on top of $\bar{f}$ (and, thus, $\bar{k}_F$) means that this quantity stems from an average with respect to an ensemble rather than to a pure state, and "cofe" stands for constant occupation factor ensemble [71], reflecting the fact that the system has the same occupation factor right up to a single (ensemble) Fermi level, unlike a polarized gas. We shall discuss below that the correct interpretation associates f_q^{cofe} with an *unpolarized* ensemble.

Before proceeding further, it is worth considering why we should choose f_q^{cofe} to be constant or zero, rather than any of the infinite number of other options we could have chosen. The main motivation is simplicity. Firstly, we aim to keep the number of parameters to two (n and $\bar{f}$) like the spin-polarized gas (n and ζ). We also aim to ensure that limiting cases (unpolarized and fully polarized gases) are reproduced by cofe gases—once adapted to inhomogeneous systems the limits respectively correspond to singlet ground states and ground and excited states of one-electron systems. Finally, noting that both limits have the special feature that they yield constant occupation factors (two and one, respectively), we aim to retain this special feature in between the limits as a sensible generalization that incorporates excited states. Crucially, Sec. IV will demonstrate that the cofe model can indeed be localized to approximate inhomogeneous states by recovering meaningful exact conditions.
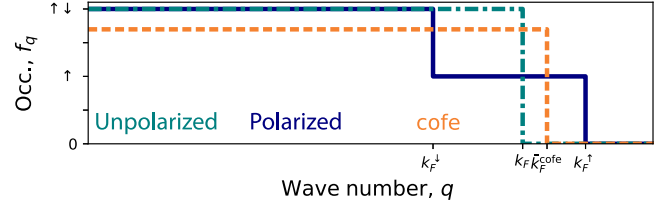

FIG. 1. Occupation (Occ.) factors as a function of wave number for an unpolarized gas (dash-dotted line), polarized gas ($\zeta = \frac{1}{2}$, solid line), and cofe gas (dashed line)—all at the same electron density.

The above goals dictate the form of Eq. (25), as well as the kinetic and exchange energies of cofe HEGs. The addition of some extra restrictions (to be discussed below, as needed) on the excited states dictates the remaining properties of cofe HEGs. As we shall see in Sec. V the resulting cofe gas is effective for predicting ground and excited states of inhomogeneous systems.

Figure 1 illustrates the different occupation factors for unpolarized, polarized, and cofe HEGs, all at the same density n. The polarized gas has $\zeta = \frac{1}{2}$, while the cofe HEG has $\bar{f} = 1.7$. The unpolarized gas has a single Fermi level with double occupations, the polarized gas has two Fermi levels, one higher ($\uparrow$) and one lower ($\downarrow$) than that of the unpolarized gas, and is doubly occupied up to the lower level and then singly occupied to the higher level. The cofe gas also has a single Fermi level between the unpolarized and $\downarrow$ levels, but is only partly occupied for all q. The choice of $\zeta = \frac{1}{2}$ and $\bar{f} = 1.7$ ensures that the polarized and cofe HEGs also have the same exchange energy—as can be seen by evaluating Eqs. (5) and (29). We will exploit this feature in Sec. III B 4.

Once we accept to deal with ensembles from constrained occupation factors, we can mix with equal weights a polarized HEG with its time-reversed partner. Nothing changes in terms of the evaluation of the energy components. What changes is the interpretation. Now we can find a continuum of unpolarized ensembles of cofe HEGs, with energies that go from that of the regular unpolarized to that of the regular fully polarized HEGs. But the ensembles can also accommodate ground states and excited states (keeping in mind that the polarized gas is itself an excited state in the absence of a magnetic field), in a sense that will be clarified just below.

The ingredients of $\hat{\Gamma}^{\text{cofe}}$ are most easily understood by considering a finite system with four electrons.

(i) The unique unpolarized state is $|\text{unpol}\rangle = |1^2 2^2\rangle$, which is consistent with a Fermi level, $\bar{k}_F^{\text{cofe}} = \epsilon_2^+$, just above the second orbital energy. As a singular state we set $w_{\text{unpol}} = 1$ and obtain $f_1 = f_2 = \bar{f} = 2$.

(ii) The fully polarized system, $|\text{fullpol}\rangle = |1^{\uparrow}2^{\uparrow}3^{\uparrow}4^{\uparrow}\rangle$, is also unique ($w_{\text{fullpol}} = 1$). It has $\bar{k}_F^{\text{cofe}} = \epsilon_4^+$ (four orbitals allowed) and yields $f_1 = f_2 = f_3 = f_4 = \bar{f} = 1$. The corresponding state with all $\downarrow$ electrons has the
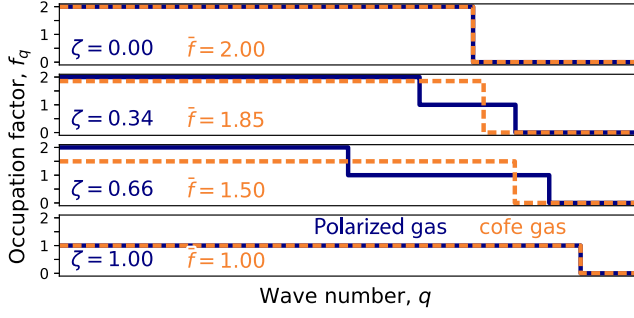
FIG. 2. Like Fig. 1 except showing polarized and cofe HEGs at a variety of ζ and $\bar{f}$. Note that the polarized and cofe gas are, as expected, the same for $\zeta = 0$ and $\bar{f} = 2$, or $\zeta = 1$ and $\bar{f} = 1$.

same energetics (but time-reversed dynamics). Ensemble averaging the $\uparrow$- and $\downarrow$-spin systems therefore yields a net unpolarized system with the same energy terms.

(iii) But, if we allow three orbitals, we have three maximally polarized ($N^\uparrow = 3$ and $N^\downarrow = 1$) states: $|\text{cofe}_0\rangle \equiv |1^2 2^\uparrow 3^\uparrow\rangle$, $|\text{cofe}_1\rangle \equiv |1^\uparrow 2^2 3^\uparrow\rangle$, and $|\text{cofe}_2\rangle \equiv |1^\uparrow 2^\uparrow 3^2\rangle$. Each state has a spin polarization $\zeta_{\text{eff}} = \frac{3-1}{4} = \frac{1}{2}$. The (noninteracting) Fermi level $k_F^\uparrow$ for $\uparrow$ electrons is always $k_F^\uparrow = \epsilon_3^+$. But we cannot define a level for $\downarrow$ electrons due to holes in $|\text{cofe}_1\rangle$ and $|\text{cofe}_2\rangle$. Assigning each of the three states an equal weight, $w_0 = w_1 = w_2 = \frac{1}{3}$, yields $f_1 = f_2 = f_3 = \frac{4}{3}$, as desired. Thus, $\bar{k}_F^{\text{cofe}} = k_F^\uparrow (= k_F^\downarrow) = \epsilon_3^+$ (after we also average over spin) for the whole ensemble.

Replacing orbital indices by q, and taking the limit $N, V \to \infty$ for fixed density, $n = (N/V)$, and ensemble Fermi level, $\bar{k}_F$, yields the actual constant occupation factor ensemble. It is composed of ground and excited states all with the same polarization, $\zeta_{\text{eff}} = 2/\bar{f} - 1$ (and their time-reversed partners), where $\bar{f} = 6\pi^2 n \bar{k}_F^{-3}$ follows from Eq. (25). Sections III B 2 and III B 4 will expand a little on the specifics of states required for cofe HEGs. Here and henceforth we drop the superscript from $\bar{k}_F^{\text{cofe}}$ and simply use $\bar{k}_F$.

It is finally worth noting that the energy of a cofe HEG with $\bar{f} = 2$ is always equal to that of an unpolarized gas with $\zeta = 0$, while the energy of a cofe HEG with $\zeta = 1$ is

always equal to that of a *fully polarized* gas with $\zeta = 1$ (keeping in mind that the ensemble averages over the time-reversed state). Figure 2 shows f_q for a selection of polarized and cofe gases between (and at) these limits, all yielding the same density, n. Values of ζ and $\bar{f}$ are "paired" to yield the same exchange energy—we will later exploit this pairing in Eq. (44) of Sec. III B 4.

We will next proceed to compute the energy components of the cofe HEG. Key results are summarized in Table I.

1. Density, kinetic, and exchange energies of cofe HEGs

The density, $n[f_q] := \int_0^\infty f_q(q^2 dq/2\pi^2)$, and kinetic energy per particle,

$$t_s[f_q] := \frac{1}{n[f_q]} \int_0^\infty f_q \frac{q^2}{2} \frac{q^2 dq}{2\pi^2}, \qquad (26)$$

of an HEG are direct functionals of the occupation factor distribution f_q. Prefactors deal with normalization of the orbitals and energies. The kinetic energy integral follows from the fact that $\phi_q^*(r)[-\frac{1}{2}\nabla^2 \phi_q(r)] = \frac{1}{2}q^2 \phi_q^*(r)\phi_q(r)$.

Typically we are interested in some fixed density, $n = (3/4\pi r_s^3)$, defined by its Wigner-Seitz radius r_s, which imposes constraints on f_q (e.g., the Fermi levels in the previous section). Throughout we will implicitly define all HEGs to be at fixed Wigner-Seitz radius r_s and vary other parameters under this assumption. Using the occupation factor model for a polarized gas with fixed ζ and r_s yields the kinetic energy given by Eq. (4).

Consider instead a cofe HEG, where f_q is given by Eq. (25). We obtain $n[f_q] = (\bar{f}\bar{k}_F^3/6\pi^2)$ from which we confirm that $\bar{k}_F = (6\pi^2 n/\bar{f})^{1/3}$. The kinetic energy of a cofe HEG therefore has the separable expression,

$$t_s^{\text{cofe}}(r_s, \bar{f}) = \frac{3\bar{k}_F(r_s, \bar{f})^2}{10} = t_s(r_s)\left[\frac{2}{\bar{f}}\right]^{2/3}, \qquad (27)$$

using $t_s(r_s)$ from Eq. (6).

In addition to the density and kinetic energy, the exchange energy of any HEG may also be evaluated directly from f_q. Replacing sums over k and k' by integrals over q and q' lets us rewrite Eq. (16) as

TABLE I. Summary of Kohn-Sham derived properties of the HEGs considered in this work. Here, $C_s = 1.10495$ and $C_x = 0.458165$. The cases $\zeta = 0$ and $\bar{f} = 2$ correspond to an unpolarized gas, and $\zeta = 1$ and $\bar{f} = 1$ are equivalent.

Type of HEG	Parameters	t_s	ϵ_x	$\Delta\epsilon_H$
Unpolarized gas	r_s	$\frac{C_s}{r_s^2}$	$\frac{-C_x}{r_s}$	0
Polarized gas	r_s, ζ	$\frac{C_s}{r_s^2}\frac{(1+\zeta)^{5/3}+(1-\zeta)^{5/3}}{2}$	$\frac{-C_x}{r_s}\frac{(1+\zeta)^{4/3}+(1-\zeta)^{4/3}}{2}$	0
Constant occupation factor ensemble (cofe)	$r_s, \bar{f}$	$\frac{C_s}{r_s^2}\left[\frac{2}{\bar{f}}\right]^{2/3}$	$\frac{-C_x}{r_s}\left[\frac{2}{\bar{f}}\right]^{1/3}$	$|\epsilon_x|\frac{(2-\bar{f})(\bar{f}-1)}{\bar{f}}$

$$\epsilon_{\rm x}[f_q] := -\frac{1}{n[f_q]}\int_0^\infty\int_0^\infty f_{\max(q,q')}V(q,q')\frac{q'^2dq'}{2\pi^2}\frac{q^2dq}{2\pi^2},$$
(28)

where $V(q,q') = \int_{-1}^1(\pi dx/q^2 + q'^2 - 2qq'x) = (\pi/qq')\times$ $\log(|q+q'|/|q-q'|)$ is the spherically averaged Coulomb potential. A little additional work on the integral (see Appendix A for details) yields Eq. (5) for a polarized gas, and

$$\epsilon_{\rm x}^{\rm cofe}(r_s,\bar{f}) = -\frac{\bar{f}}{n}\int_0^{\bar{k}_F}\frac{q}{\pi}\frac{q^2dq}{2\pi^2} = \epsilon_{\rm x}(r_s)\left[\frac{2}{\bar{f}}\right]^{1/3}$$
(29)

for cofe HEGs, where $\epsilon_{\rm x}(r_s)$ is the unpolarized HEG expression of Eq. (7).

Although not necessary for computing $\epsilon_{\rm x}$, we may similarly derive an expression for the HEG exchange hole, defined in Eq. (21). We obtain

$$n_{2,{\rm x}}^{\rm cofe}(R;r_s,\bar{f}) = \Pi_{\rm x}^{\rm cofe}(r_s,\bar{f})N(\bar{k}_FR),$$
(30)

where

$$\Pi_{\rm x}^{\rm cofe}(r_s,\bar{f}) = -\bar{f}\int_0^{\bar{k}_F}\frac{q^3}{3\pi^2}\frac{q^2dq}{2\pi^2} = \frac{-n^2}{\bar{f}}$$
(31)

is the on-top pair density of the exchange hole and $N(x) := 9[\sin(x) - x\cos(x)]^2/x^6$ is a function. We will use the relationship between the exchange energy and exchange hole to help in deriving the properties of the Hartree energy in the next section.

2. Hartree energy of cofe HEGs

The ensemble Hartree energy functional is given in Eq. (15). This term is usually ignored in HEG discussions because $n_{2,{\rm H}} = n^2$ in polarized and unpolarized gases at arbitrary ζ, which means that $\epsilon_{\rm H}$ exactly cancels the energy of the positive background charge, $\epsilon_{\rm bg}$—that is, $\epsilon_{\rm H}[n_{2,{\rm H}} = n^2] = -\epsilon_{\rm bg}$. In cofe HEGs this cancellation is incomplete. The singular background charge is guaranteed, by charge neutrality, to be canceled in full. However, the Hartree pair density, $n_{2,{\rm H}}^w \neq n^2$, differs from the background charge density n^2, and thus $\epsilon_{\rm H}^w$ includes additional terms. The energy per particle of an ensemble HEG is

$$e^w[f_q^w] := t_s[f_q^w] + \Delta\epsilon_{\rm H}^w[f_q^w] + \epsilon_{\rm x}[f_q^w] + \epsilon_{\rm c}^w[f_q^w],$$
(32)

where superscripts w indicate an explicit dependence on the nature of the ensemble. The additional positive Hartree energy contribution,

$$\Delta\epsilon_{\rm H}^w = \epsilon_{\rm H}^w - \epsilon_{\rm bg} = \frac{1}{n}\int\Delta n_{2,{\rm H}}^w(R)\frac{d{\bf R}}{2R},$$
(33)

may be evaluated [Eqs. (19) and (20)] using the ensemble Hartree pair-density deviation, $\Delta n_{2,{\rm H}}^w = n_{2,{\rm H}}^w - n^2$.

We therefore seek closed-form expressions for $n_{2,{\rm H}}^{\rm cofe}$ and $\Delta\epsilon_{\rm H}^{\rm cofe}$ for the special case of a cofe HEG with maximal polarization within the ensemble, as defined earlier. Full details for Hartree expressions are rather involved so have been left to Appendix B. The rough argument is as follows: (1) the background charge is canceled by $\kappa = \kappa'$ terms in Eq. (15) or (20), so we need only evaluate $\kappa \neq \kappa'$ terms, (2) the cofe states $|\kappa\rangle$ contain every possible combination of paired and unpaired orbitals up to $\bar{k}_F$, (3) each of these states is weighted equally, and (4) we may therefore use combinatorial arguments to evaluate key expressions. The final step recognizes that each state may be defined by a set, $\{q\}_{\rm double}$, of doubly occupied orbitals, such that the remaining occupied orbitals (with $|q| \leq \bar{k}_F$) contain only an ↑ electron. Each noninteracting state is then a Slater determinant consistent with the occupations, whose properties may be understood via $\{q\}_{\rm double}$ and $\bar{k}_F$.

Appendix B yields $\Delta\epsilon_{\rm H}^{\rm cofe}(r_s,\bar{f}) := \frac{C_{\rm H}}{r_s}\frac{(2-\bar{f})(\bar{f}-1)}{\bar{f}^{4/3}}$ [Eq. (B8)], where $C_{\rm H} = 2^{1/3}C_{\rm x}$. We rewrite this as

$$\Delta\epsilon_{\rm H}^{\rm cofe}(r_s,\bar{f}) = |\epsilon_{\rm x}(r_s,\bar{f})|\frac{(2-\bar{f})(\bar{f}-1)}{\bar{f}}$$
(34)

for use in Eq. (32) and later expressions. This result follows from the fact that

$$n_{2,{\rm H}}^{\rm cofe}(R;r_s,\bar{f}) = n^2 + \Delta\Pi_{\rm H}^{\rm cofe}(r_s,\bar{f})N(\bar{k}_FR),$$
(35)

$$\Delta\Pi_{\rm H}^{\rm cofe}(r_s,\bar{f}) = n^2\frac{(2-\bar{f})(\bar{f}-1)}{\bar{f}^2}$$

$$= -\frac{(2-\bar{f})(\bar{f}-1)}{\bar{f}}\Pi_{\rm x}^{\rm cofe},$$
(36)

where $N(x)$ is the same expression used in Eq. (30).

3. Energies in the low-density limit of cofe HEGs

We cannot analytically evaluate the energy of an HEG at arbitrary density n. We can, however, semianalytically evaluate it in the high-density (large n, small r_s) and low-density (small n, large r_s) limits. The high-density limit may be obtained from a series solution around the Kohn-Sham solution. In the low-density limit, the electrons are far enough apart to undergo a process known as a Wigner crystallization [72,73]. The resulting "strictly correlated electron" physics may then be understood via a classical leading order term, with quantum corrections. The transition occurs at $r_s \approx 100$ bohr.

Recent work [50] has shown that any dependence on ensemble properties must vanish in the low-density limit of any finite system, so that all excited-state properties become degenerate to both leading and subleading order.

It is very likely that this result also holds true in the thermodynamic limit of HEGs, as justified by the following intuition.

(1) As the density becomes small, the distance between electrons becomes large and the particles become effectively classical with a quantum state defined by fluctuations around a classical minima.

(2) Whether the system is finite or infinite, the fluctuations may be "excited" any number of times with no impact on the *classical* leading order term of the interaction energy.

(3) Furthermore, the next leading order *quantum* correction from zero-point energy fluctuations around the classical minima are dictated only by the density constraint, and are therefore also independent of excitation structure.

This result has important implications for both spin-polarized and cofe HEGs, as both may be represented as ensemble of excited states—with specific properties governed by ζ or $\bar{f}$, respectively. It follows from the above that the leading two orders of their low-density energies are independent of the excitation structure. Consequently, energies are independent of $\bar{f}$ and ζ. Independence of ζ has long been theorized for spin-polarized HEGs. Recent QMC data [74] provide confirmation of this result.

The leading order terms correspond to $1/r_s$ and $1/r_s^{3/2}$ in the usual large-r_s series description of HEGs. Therefore, ensemble and spin effects can only contribute at $O(1/r_s^2)$. The (Hartree) exchange and correlation energy of strictly correlated electrons in the low-density limit (ld) therefore obeys $\lim_{r_s \to \infty} \epsilon_{\mathrm{Hxc}}(r_s, \zeta) = \epsilon_{\mathrm{Hxc}}^{\mathrm{ld}}(r_s)$, where

$$\epsilon_{\mathrm{Hxc}}^{\mathrm{ld}}(r_s) := \frac{-C_\infty}{r_s} + \frac{C_\infty'}{r_s^{3/2}} + \cdots \tag{37}$$

includes only the part of the Hartree energy that is not canceled by background charge. The best estimates for coefficients are $C_\infty = 0.8959 \approx 1.95 C_\mathrm{x}$ and $C_\infty' = 1.328$ [75,76].

In regular HEGs, the Hartree term is fully canceled by background charge and so can be ignored. For polarized HEGs we therefore obtain $\lim_{r_s \to \infty} \epsilon_c = \epsilon_{\mathrm{Hxc}}^{\mathrm{ld}} - \epsilon_\mathrm{x}$ and

$$\lim_{r_s \to \infty} \epsilon_c(r_s, \zeta) := \frac{-C_\infty + C_\mathrm{x} f_\mathrm{x}(\zeta)}{r_s} + \frac{C_\infty'}{r_s^{3/2}} + \cdots, \tag{38}$$

using f_x from Eq. (5). By contrast, in a cofe HEG there is a nonzero component $(\Delta \epsilon_\mathrm{H}^{\mathrm{cofe}})$ in the Hartree energy. It therefore follows that $\lim_{r_s \to \infty} \epsilon_c^{\mathrm{cofe}} = \epsilon_{\mathrm{xc}}^{\mathrm{ld}} - \Delta \epsilon_\mathrm{H}^{\mathrm{cofe}} - \epsilon_\mathrm{x}^{\mathrm{cofe}}$. We finally obtain

$$\lim_{r_s \to \infty} \epsilon_c^{\mathrm{cofe}}(r_s, \bar{f}) = \frac{-C_\infty + C_\mathrm{x} f_{\mathrm{Hx}}^{\mathrm{cofe}}(\bar{f})}{r_s} + \frac{C_\infty'}{r_s^{3/2}} + \cdots, \tag{39}$$

where

$$f_{\mathrm{Hx}}^{\mathrm{cofe}}(\bar{f}) = \left[\frac{2}{\bar{f}}\right]^{1/3} \frac{(\bar{f} - 1)^2 + 1}{\bar{f}} \tag{40}$$

follows from Eqs. (29) and (34). This is the appropriate low-density series expansion for the correlation energy of cofe HEGs.

4. State-driven correlation energies of cofe HEGs

In general, the correlation energy of an ensemble is separable into two terms [47–49], $E_c^w := E_c^{\mathrm{SD},w} + E_c^{\mathrm{DD},w}$ [Eq. (17)], where each covers different physics of the ensemble. The state-driven term is the only term present in pure states, such as polarized gases. In general ensembles, it is like a weighted average of conventional correlation energies for the different states of the ensemble. The density-driven term reflects the fact that the densities of the individual Kohn-Sham and interacting states that form the ensemble are not necessarily the same—only the averaged ensemble density is the same.

We expect that only the SD part of the correlation energy should form part of the xc energy used in density functional approximations, so we focus here on this term—we explain this choice in Sec. IV. Our goal is therefore to determine $\epsilon_c^{\mathrm{SD,cofe}}(r_s, \bar{f})$ as a function of r_s and $\bar{f}$, which we will use as a basis for parametrization in the next section. This involves considering the high- and low-density limits of matter (and therefore cofe HEGs), for which exact results will be derived. We will also discuss how to repurpose existing data for values in between these limits. Comprehensive analysis of both state- and density-driven correlation terms is reported in Appendix C. Below, we summarize key elements of the SD correlation energy analysis.

The division into SD and DD terms is not unique [47–49], and any explicit study of the separation into SD and DD terms requires accessing the properties of a variety of excited states of *interacting* HEGs. Nevertheless, discussion near Eq. (14) of [49] argues that the SD correlation energy may be written in adiabatic connection and fluctuation-dissipation (ACFD) theorem form:

$$\epsilon_c^{\mathrm{SD}} := \frac{1}{n} \int_0^1 d\lambda \int_0^\infty \frac{-d\omega}{\pi} \int \frac{d\mathbf{r} d\mathbf{r}'}{2|\mathbf{r} - \mathbf{r}'|} \\ \times [\chi_\lambda(\mathbf{r}, \mathbf{r}'; i\omega) - \chi_0(\mathbf{r}, \mathbf{r}'; i\omega)], \tag{41}$$

which is Eq. (18) adapted to HEGs. Here, χ_0 is the collective density-density response of the noninteracting cofe HEG defined earlier—i.e., the ensemble of part-polarized ground and excited states that yield $\bar{f}$. χ_λ is its equivalent for a scaled Coulomb interaction $(1/R) \to (\lambda/R)$. In principal, the individual states in the interacting ensemble may be followed from their known $\lambda = 0$ values to their unknown value at arbitrary λ, although this is not required in practice.

The key step toward understanding how to separate and parametrize terms is to use the random-phase

approximation (RPA). RPA becomes exact (to leading order) in the high-density limit [10]. More generally, RPA provides an approximate solution for Eq. (41), and thus provides insights into the SD correlation term. Details are provided in Appendix C 1. Key findings are that (i) $\epsilon_c^{\text{SD,cofe}}$ is approximately linear in $\bar{f}$ for high densities and (ii) for low densities we obtain a scaling that is similar to $f_x^{\text{cofe}}(\bar{f})$. Appendix C 2 then uses the RPA results and fundamental theory to argue that

$$\epsilon_c^{\text{SD,cofe,hd}}(r_s, \bar{f}) = (\bar{f} - 1)\epsilon_c(r_s, 0) + (2 - \bar{f})\epsilon_c(r_s, 1), \quad (42)$$

$$\epsilon_c^{\text{SD,cofe,ld}}(r_s, \bar{f}) = \epsilon_x(r_s)\left[\frac{C_\infty}{C_x} - f_x^{\text{cofe}}(\bar{f})\right] + \frac{C_\infty'}{r_s^{3/2}} \quad (43)$$

are, respectively, the exact high- and low-density limits of ϵ_c^{cofe}. That is, $\lim_{r_s \to 0} \epsilon_c^{\text{SD,cofe}}(r_s, \bar{f}) = \epsilon_c^{\text{SD,cofe,hd}}(r_s, \bar{f})$ and $\lim_{r_s \to \infty} \epsilon_c^{\text{SD,cofe}}(r_s, \bar{f}) = \epsilon_c^{\text{SD,cofe,ld}}(r_s, \bar{f})$.

Filling in the gaps between these limits requires QMC calculations, which, however, are available only for spin-polarized ground states of homogeneous gases. Appendix C 2 therefore shows how to reuse existing spin-polarized QMC data for the in-between regime, by adapting it for cofe HEGs. Specifically, it argues that

$$\epsilon_c^{\text{SD,cofe,mhd}}(r_s, \bar{f}) \equiv \epsilon_c^{\text{QMC}}(r_s, \zeta = \hat{f}_{\text{x-map}}^{-1}(\bar{f})) \quad (44)$$

is a reasonable *approximation* for medium-high densities (mhd). The key assumption behind this relationship is that HEGs with same exchange energy should have a similar state-driven correlation energy. Thus, $\hat{f}_{\text{x-map}}(\zeta)$ is a function yielding $\epsilon_x^{\text{cofe}}(r_s, \hat{f}_{\text{x-map}}(\zeta)) = \epsilon_x(r_s, \zeta)$ and $\epsilon_x^{\text{cofe}}(r_s, \bar{f}) = \epsilon_x(r_s, \hat{f}_{\text{x-map}}^{-1}(\bar{f}))$. Equation (44) becomes exact in the low-density limit, but incorrect in the high-density limit. More information is provided in Appendix C 2.

Appendix D details parametrization of $\epsilon_c^{\text{SD,cofe}}(r_s, \bar{f})$ for arbitrary densities, based on the theoretical work in this section. As an intermediate step, it also introduces approximations for $\hat{f}_{\text{x-map}}$ and its inverse, for use in Eq. (44). Key results are visually summarized in Fig. 3, which compares the parametrization of $\epsilon_c^{\text{SD,cofe}}$ with the (adapted) reference data used to fit it. The top plot shows correlation energies, $\epsilon_c^{\text{SD,cofe}}(r_s, \bar{f})$. The middle plot shows deviations, $\Delta\epsilon_{\text{xc}}^{\text{SD,cofe}} = \epsilon_{\text{xc}}^{\text{SD,cofe}}(r_s, \bar{f}) - \epsilon_{\text{xc}}^{\text{SD,cofe}}(r_s, 2)$, from unpolarized gas values. The bottom plot shows xc enhancement factors, $\epsilon_{\text{xc}}^{\text{SD,cofe}}(r_s, \bar{f})/\epsilon_{\text{xc}}^{\text{SD,cofe}}(r_s, 2)$, which must approach one (100%) in the low-density (large r_s) limit.

IV. FROM cofe HEGs TO REAL SYSTEMS

As discussed in Sec. II B, Kohn and Sham used an inhomogeneous description of the (quantum mechanical) kinetic and (classical) Hartree energies, together with an
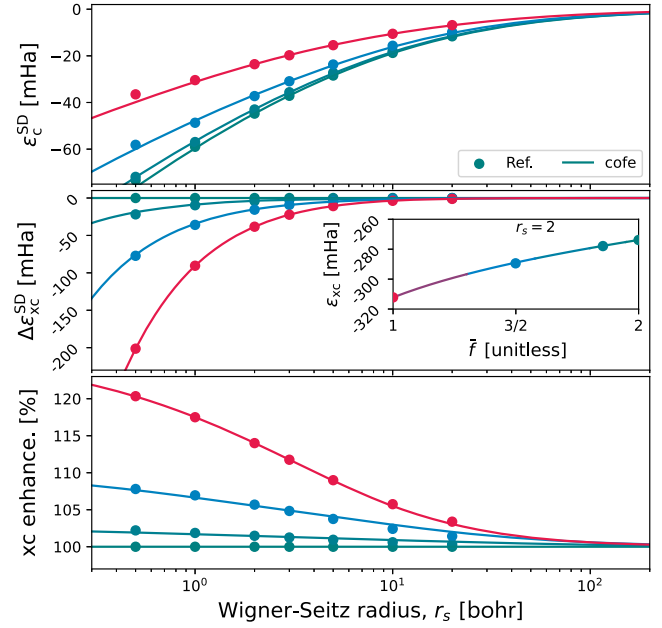

FIG. 3. Correlation (top) and xc (middle) energies and xc (bottom) enhancement factors for HEGs as a function of r_s and $\bar{f} \in (2, 1.85, 1.50, 1)$. Plots show the cofe (solid lines) parametrization introduced here and the adapted benchmark results from Ref. [8] (circles). The inset shows ϵ_{xc} (cofe and benchmark) as a function of $\bar{f}$, for $r_s = 2$. Line colors indicate the value of $\bar{f}$ (see inset for values).

HEG-based approximation for the exchange and correlation energy only, per Eq. (9). It is natural to assume that ensembles and excited states can benefit from a similar treatment. However, for ensembles it is important to work with the corresponding *extended* functionals and, in particular, the Hartree functional forms described in Eq. (15). Recent applications have confirmed the advantages of using Eq. (15), rather than the traditional classical electrostatic energy [43–45].

Switching to ensemble of excited states, and mimicking Eq. (9) to employ the cofe HEGs, leads to

$$E_{\text{eLDA}}^w = \min_n \left\{ T_s^w[n] + \int n(\boldsymbol{r})v(\boldsymbol{r})d\boldsymbol{r} + E_{\text{H}}^w[n] \right.$$
$$\left. + \int n(\boldsymbol{r})\epsilon_{\text{xc}}^{\text{cofe}}(r_s(\boldsymbol{r}), \bar{f}(\boldsymbol{r}))d\boldsymbol{r} \right\}. \quad (45)$$

Here, we have replaced pure state T_s and E_{H} by their ensemble equivalents, T_s^w [Eq. (14)] and E_{H}^w [Eq. (15)], and locally approximated the xc energy by the cofe LDA with *local* Wigner-Seitz radius $r_s(\boldsymbol{r})$ and *local* effective occupation factor $\bar{f}(\boldsymbol{r})$. Note, as was done earlier, we leave *w* superscripts off local quantities (n, r_s, and $\bar{f}$).

Furthermore—and much more useful in practice—it is possible to use Eq. (45) to generate state-resolved

energies $E_{|\kappa\rangle}$ for target states $|\kappa\rangle$ [77] that obey stationary conditions [78]. The resulting eLDA energy expression is

$$E^{\mathrm{eLDA}}_{|\kappa\rangle} = T_{s,|\kappa\rangle}[n_{|\kappa\rangle}] + \int n_{|\kappa\rangle}(\boldsymbol{r})v(\boldsymbol{r})d\boldsymbol{r} + E_{\mathrm{H},|\kappa\rangle}[n_{|\kappa\rangle}]$$

$$+ \int n_{|\kappa\rangle}(\boldsymbol{r})\epsilon^{\mathrm{cofe}}_{\mathrm{xc}}(r_{s,|\kappa\rangle}(\boldsymbol{r}),\bar{f}_{|\kappa\rangle}(\boldsymbol{r}))d\boldsymbol{r}. \quad (46)$$

In brief, Eq. (46) follows from applying the exact weight-derivative relationship, $E_{|\kappa\rangle} = \partial_{w_\kappa}E^w$ [for any positive weight w_κ in the ensemble; see Eq. (11)], to the eLDA energy expression, after assuming that orbitals are fixed in the derivative [44]. $T_{s,|\kappa\rangle}$ and $E_{\mathrm{H},|\kappa\rangle}$ are obtained from the inhomogeneous system. We approximate the exchange and state-driven correlation energy via

$$\epsilon^{\mathrm{cofe}}_{\mathrm{xc}}(r_s,\bar{f}) := \epsilon^{\mathrm{cofe}}_{\mathrm{x}}(r_s,\bar{f}) + \epsilon^{\mathrm{SD,cofe}}_{\mathrm{c}}(r_s,\bar{f}) \quad (47)$$

from the local Wigner-Seitz radius $r_{s,|\kappa\rangle}(\boldsymbol{r})$ and local effective occupation factor $\bar{f}_{|\kappa\rangle}(\boldsymbol{r})$. We will discuss energy terms in the next subsection and return to $\bar{f}$ in Sec. IV B.

A. State-resolved treatment

In the state-resolved treatment, each excited state $|\kappa\rangle$ is dictated by a set of orbital occupancies and spin symmetry (singlet, doublet, triplet, etc)—in weakly correlated wave functions these would indicate the dominant Slater determinants in a configuration expansion of the true excited state. Both $T_{s,|\kappa\rangle}$ and $n_{s,|\kappa\rangle}$ take their usual forms, but with orbital occupation factors $\theta^{|\kappa\rangle}_i$ taken from the excited state. The Hartree energy is obtained from Eq. (15) to yield

$$E_{\mathrm{H},|\kappa\rangle} := \partial_{w_\kappa}E^w_{\mathrm{H}} \equiv U[n_{|\kappa\rangle}] + 2\sum_{\kappa'<\kappa}U[n_{s,\kappa\kappa'}]. \quad (48)$$

The first term is the typical ground state Hartree energy, $E_{\mathrm{H}}[n_{|\kappa\rangle}] = U[n_{|\kappa\rangle}]$, but the extra $U[n_{s,\kappa\kappa'}]$ terms involve the Coulomb energy of a transition density from KS state $|\kappa_s\rangle$ to a lower energy KS state $|\kappa'_s\rangle$ of the same symmetry, i.e., "deexcitations," For the lowest-lying excitation of each given symmetry (spatial or spin) a standard-looking pure state problem is well defined, but complications appear when considering higher excitations.

This work considers only the lowest energy excitation for each allowed symmetry, and some other symmetry-protected excited states, and thus solves Eq. (46) via minimization. Specifically, it considers three types of excited states, whose KS states may be fully defined via electron promotion ($\hat{P}^{\mathrm{to}}_{\mathrm{from}}$) from the lowest energy doubly occupied singlet state, $|S_0\rangle$: single excitation (promotion) to a triplet,

$$|T^a_i\rangle \equiv \frac{1}{\sqrt{2}}[\hat{P}^{a\uparrow}_{i\uparrow} - \hat{P}^{a\downarrow}_{i\downarrow}]|S_0\rangle,$$

single excitation (promotion) to a singlet,

$$|S^a_i\rangle \equiv \frac{1}{\sqrt{2}}[\hat{P}^{a\uparrow}_{i\uparrow} + \hat{P}^{a\downarrow}_{i\downarrow}]|S_0\rangle,$$

and double excitation (promotion) to a singlet,

$$|S^{a^2}_{i^2}\rangle \equiv \hat{P}^{a\uparrow}_{i\uparrow}\hat{P}^{a\downarrow}_{i\downarrow}|S_0\rangle.$$

Thus, once we define each state via i, a, and the nature of the excitation, we are able to find the eLDA energy by minimizing Eq. (46) with respect to orbitals using the approach detailed in Sec. II of Supplemental Material [79]. Orbital self-consistent solutions $\{\phi^{|\kappa\rangle}_i\}$ are therefore different in each state $|\kappa\rangle$.

The xc energy approximation is detailed in Appendix D. The exchange energy term takes the exact (for cofe gases) form,

$$\epsilon^{\mathrm{cofe}}_{\mathrm{x}}(r_s,\bar{f}) := \epsilon_{\mathrm{x}}(r_s)[2/\bar{f}]^{1/3}, \quad (49)$$

while the state-driven correlation energy term may be parametrized as

$$\epsilon^{\mathrm{SD,cofe}}_{\mathrm{c}}(r_s,\bar{f}) := (\bar{f}-1)\epsilon^0_{\mathrm{c}} + (2-\bar{f})\epsilon^1_{\mathrm{c}}$$

$$+ (\bar{f}-1)(2-\bar{f})\left[M_2(r_s) + \left(\frac{3}{2}-\bar{f}\right)M_3(r_s)\right] \quad (50)$$

for $\epsilon^\zeta_{\mathrm{c}}$ computed using Eq. (D4) (parameters in Table II). Here, $M_{2,3}(r_s)$ involve weighted sums (coefficients in Table III) over functions $\epsilon^\zeta_{\mathrm{c}}$.

Finally, we stress that Eq. (46) ignores density-driven correlations entirely, i.e., sets $E^{\mathrm{DD},w}_{\mathrm{c}} \equiv 0$. This is because DD correlations, like Hartree interactions (either regular or ensemblized), are highly nonlocal quantities [see Eq. (22)] that must not be treated via *any* LDA. Ignoring DD correlation should not significantly affect our conclusions, as supported by the close agreement between time-dependent LDA (TDLDA) and eLDA on single particle excitations in Sec. V.

B. Effective occupation factor

The final step toward the eLDA is to justify and derive a local effective occupation factor. Equation (46) assumes that exchange and state-driven correlations may be approximated locally. In fact, we know from recent works [44,45] that excited-state physics can be modeled effectively by reusing ground state semilocal xc approximations, because applying combination rules [44] to existing DFAs can be very effective in practice. Physically, this may be justified by recognizing that exchange and state-driven correlations

TABLE II. Correlation energy parameters for selected values of ζ from fits to benchmark data [8] and exact constraints.

ζ^{QMC}	A	α	β_1	β_2	β_3	β_4
			cofe parameters			
0.00	0.031 091	0.1825	7.5961	3.5879	1.2666	0.4169
0.34	0.028 833	0.2249	8.1444	3.8250	1.6479	0.5279
0.66	0.023 303	0.2946	9.8903	4.5590	2.5564	0.7525
1.00	0.015 545	0.1260	14.1229	6.2011	1.6503	0.3954
			rPW92 parameters			
0.00	0.031 091	0.1825	7.5961	3.5879	1.2666	0.4169
0.34	0.030 096	0.1842	7.9233	3.7787	1.3510	0.4326
0.66	0.026 817	0.1804	9.0910	4.4326	1.5671	0.4610
1.00	0.015 546	0.1259	14.1225	6.2009	1.6496	0.3952

TABLE III. Weighted sum parameters for $M_{2,3}$ (Appendix D) and $Z_{2,3}$ (Appendix E). For example, $M_2 = -2\epsilon_c^0 + 4\epsilon_c^{0.66} - 2\epsilon_c^1$ and $Z_3 = 19.86\epsilon_c^0 - 30.57\epsilon_c^{0.34} + 12.71\epsilon_c^{0.66} - 2\epsilon_c^1$.

Function	ϵ_c^0	$\epsilon_c^{0.34}$	$\epsilon_c^{0.66}$	ϵ_c^1
		cofe parameters		
M_2	−2.00	0.00	4.00	−2.00
M_3	13.33	−22.41	11.43	−2.35
		rPW92 parameters		
Z_2	−10.95	13.32	−1.47	−0.90
Z_3	19.86	−30.57	12.71	−2.00

are response-based properties [49] and are thus consistent [81] with "xc hole-based" approximations [56].

We therefore see that even the regular LDA (and extensions) *can* be reused. Thus it is natural to expect that the cofe gas—which accounts for the excited states of jellium—can do even better. But how do we localize the energy of the cofe gas? The first step toward an answer is to recognize that the exact exchange energy density of ensembles or excited states depends only on the orbitals $\{\phi_i\}$ and their occupations $\{f_i\}$ [49], which can be seen by rewriting Eq. (16) as $E_x^w := \int n(\mathbf{r})\epsilon_x^{\mathrm{exact}}(\mathbf{r}, \{f_i^w\})d\mathbf{r}$, where

$$\epsilon_x^{\mathrm{exact}}(\mathbf{r}, \{f_i\}) := -\frac{1}{2}\sum_i \frac{f_i n_i(\mathbf{r})}{n(\mathbf{r})}$$
$$\times \left\{ v_U[n_i](\mathbf{r}) + 2\mathrm{Re}\sum_{i'<i} \frac{n_{ii'}(\mathbf{r})}{n_i(\mathbf{r})} v_U[n_{i'i}](\mathbf{r}) \right\},$$
$$(51)$$

using $n_{ii'} = \phi_i \phi_{i'}^*$ and $v_U[n] = \int n(\mathbf{r}')(d\mathbf{r}'/|\mathbf{r}-\mathbf{r}'|)$. Furthermore, because combination rule ensemble DFAs (eDFAs) are effective for x and c, and depend only on local densities [44], we know we can use orbital densities, $n_i = |\phi_i|^2$, instead of orbitals. Thus, $\epsilon_{\mathrm{xc}}(\mathbf{r}) \approx \epsilon_{\mathrm{xc}}(\{n_i(\mathbf{r})\}, \{f_i\})$ is a viable approximation.

The second step is to consider limiting cases. The motivation behind cofe gases (per Sec. III B) is to replace ζ by $\bar{f}$ as an interpolative variable between unpolarized and fully polarized physics, as the simplest extension of HEGs with minimal bias to spin physics. By construction, this model should naturally capture two limiting cases for eLDAs: (i) LSDA should be reproduced for the doublet ground state xc energy of any one-electron system (where $\zeta = 1$ and $\bar{f} = 1$ are unambiguous) and (ii) LDA should be reproduced in unpolarized ground states (where $\zeta = 0$ and $\bar{f} = 2$ are unambiguous). Another natural limiting case is the cofe HEG itself. We can capture these limiting cases by writing $\epsilon_{\mathrm{xc}}(\{n_i(\mathbf{r})\}, \{f_i\}) \approx \epsilon_{\mathrm{xc}}^{\mathrm{cofe}}(n(\mathbf{r}), \bar{f}(\mathbf{r}))$, where $\bar{f}(\mathbf{r}) = \bar{f}(\{f_i\}, \{n_i(\mathbf{r})\})$ is a local mapping (approximation) for ground and excited states that is constrained in form to reproduce known limits.

Thus, we make an ansatz for $\bar{f}(\{f_i\}, \{n_i(\mathbf{r})\})$ that is correct, by construction, for limiting cases but that—as we will show below—is also effective for inhomogeneous systems. As anticipated at the beginning of this section, it is convenient to switch from a state-average to a state-resolved approach. A first natural ansatz is thus the density-weighted average of occupation factors,

$$\bar{f}_{\mathrm{wocc}}^{|\kappa\rangle}(\mathbf{r}) := \sum_i \theta_i^{|\kappa\rangle} \frac{\theta_i^{|\kappa\rangle} n_i(\mathbf{r})}{n(\mathbf{r})} = \frac{\sum_i (\theta_i^{|\kappa\rangle})^2 n_i(\mathbf{r})}{\sum_i \theta_i^{|\kappa\rangle} n_i(\mathbf{r})}, \quad (52)$$

expressed here for a given excited state $|\kappa\rangle$ (we replace $\theta_i^{|\kappa\rangle}$ by f_i^w in ensembles). Here, $n_i = |\phi_i|^2$ is the density of orbital ϕ_i, and $\theta_i^{|\kappa\rangle}$ is its occupation factor in $|\kappa\rangle$. It is easily verified that this ansatz is exact for the cofe HEG, unpolarized and one-electron cases, so is *prima facie* a reasonable extension to inhomogeneous systems. However, testing (to be discussed below) reveals that this ansatz can yield poor results for ground states. These errors come from the effective spin enhancement being too great in regions that are partly polarized [i.e., where $1 < \bar{f}(\mathbf{r}) < 2$]. Fortunately, we may exploit the fact that there are other

choices of inhomogeneous $\bar{f}(\boldsymbol{r})$ that yield correct limits, but that do not hamper performance in inhomogeneous ground states.

We therefore (see Sec. I of Supplemental Material [79] for details) instead adopt an empirical double weighted average,

$$\bar{f}_{\mathrm{dwocc}}^{|\kappa\rangle}(\boldsymbol{r}) := \frac{\sum_i (\theta_i^{|\kappa\rangle})^{1/3} n_i(\boldsymbol{r})}{\sum_i \theta_i^{|\kappa\rangle} n_i(\boldsymbol{r})} \frac{\sum_i (\theta_i^{|\kappa\rangle})^{8/3} n_i(\boldsymbol{r})}{\sum_i \theta_i^{|\kappa\rangle} n_i(\boldsymbol{r})}, \quad (53)$$

for calculations. Here, in addition to satisfying exact limits, Eq. (53) also approximately replicates the LSDA in general doublet systems. Compliance with this constraint is justified by the fact that Eq. (51) is exact for spin-polarized ground states [44], which therefore provides a norm for general excited-state physics.

The left-hand panel of Fig. 4 illustrates the importance of choosing $\bar{f}$ appropriately. It shows the exchange enhancement factor of a doublet system (density $n = 2n_{\mathrm{core}} + n_{\mathrm{frontier}}$ so that $\theta_{\mathrm{core}} = 2$ and $\theta_{\mathrm{frontier}} = 1$), for different ratios of $n_{\mathrm{frontier}}/n_{\mathrm{core}}$, using standard spin polarization, and ensemble enhancement with Eqs. (52) and (53). It is clear that Eq. (52) overenhances exchange in general, relative to LSDA. By contrast, Eq. (53) matches quite closely to the spin-polarized enhancement of LSDA for all ratios.

V. APPLICATIONS

A. Ground states

How well does eLDA work in practice? The next section will address excited state energies. But, first, we need to ensure that the eLDA does not make things worse for ground state energies. The right-hand panel of Fig. 4 therefore shows the ionization potentials (IPs) of atoms—that is, the difference in ground state energies between the atom and its cation—computed with Eq. (45) using Eqs. (52) and (53). IPs provide a useful test of $\bar{f}(\boldsymbol{r})$ on ground states because the occupation factors of atoms and ions are always different and at least one system always involves an unpaired electron.
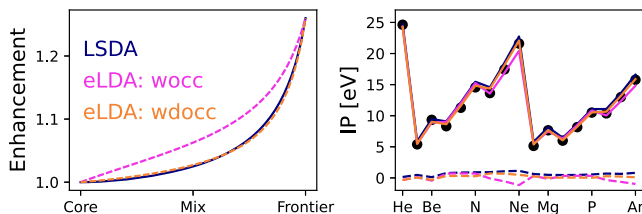
Figure 4 reveals that Eq. (53) yields results that are consistently close to standard LSDA calculations, whereas Eq. (52) leads to much greater deviations in some cases. We therefore see that using Eq. (53) yields good (relative to LSDA) performance on ground states, and we use Eq. (53) for our inhomogeneous effective occupation factor in all subsequent calculations.

Technical details for all atomic and molecular calculations for ground and excited states are in Sec. II of Supplemental Material [79]. For now it suffices to say that we carry out LSDA and TDLDA calculations using standard self-consistent field (SCF) approaches implemented in PSI4 [82,83] and PYSCF [84,85], but evaluate eLDA calculations using an orbital optimized approach with psi4 as an "engine." Spin and spatial symmetries are preserved in eLDA calculations, except for atoms which are evaluated using cylindrical spatial symmetries for consistency with standard quantum chemistry codes and practice.

B. Low-lying excitations in molecules

With the eLDA established and validated on ground state systems, we are ready to test its predictive ability for excitations. As a first test (Fig. 5), we consider the 12 triplet-singlet gaps in biradicals of the TS12 [86] dataset. The performance of Perdew and Wang's (PW92) HEG parametrization [10] energy differences (referred to as ΔSCF calculations, to differentiate from TDLDA calculations) on this dataset was explored in [87], using restricted, unrestricted, and complex orbital Kohn-Sham theory. The mean-signed errors (root mean squared errors) from ΔSCF calculations are -13.7 (14.5) kcal/mol using LSDA (i.e., unrestricted Kohn-Sham theory) and 10.9 (11.5) kcal/mol for restricted theory. Employing complex orbitals reduces these LDA errors substantially, to -1.2 (2.2) kcal/mol, albeit at the expense of nonidempotent density matrices.

Using the eLDA formalism developed here (also a ΔSCF method) to compute the gaps yields errors of -5.0 (7.4) kcal/mol—respectable statistics and a major improvement on LSDA, as shown in Fig. 5. Indeed, eLDA is closer in quality to the complex orbital performance than LDA or LSDA performance, despite eLDA being a heavily

FIG. 4. Left: doublet enhancement factor for different ratios of core and frontier occupied orbitals from LSDA (teal) and eLDA with effective $\bar{f}$ from Eq. (52) (wocc, magenta) and Eq. (53) (wdocc, orange). Right: ionization potentials (IPs) for atoms He-Ar using a conventional LSDA [9] (navy), Eq. (52) (magenta), and Eq. (53) (orange). Dashed lines indicate deviations from experimental IPs.
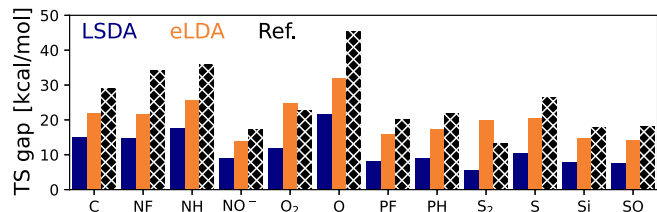

FIG. 5. Triplet-singlet gaps in atoms and diatomic systems from LSDA (navy) and eLDA (orange) calculations, compared to experimental reference data (black with crosses). LSDA and reference data from Ref. [87]. TDLDA gaps are too large for the figure, so have been left out.

constrained "restricted" theory that preserves idempotency (unlike complex orbitals) and avoids spin-contamination issues (unlike unrestricted KS). This is in partial contrast to the common [88] expectation that symmetry breaking helps DFAs to capture difficult physics. TDLDA (using VWN correlation [9] and starting from the triplet ground states for consistency with other results) yields enormous errors of 77.2 (88.6) kcal/mol—too large to include in the figure. eLDA thus outperforms both ground state (LSDA) and excited-state (TDLDA) LDA-based calculations.

Continuing on the theme of predicting difficult excitations, let us consider some excitations that TDLDA cannot predict at all: double excitations. Double excitations are singlet excited states in which the interacting wave function is dominated by a Slater determinant with paired orbitals, and in which one pair is "doubly promoted" from the dominant ground state Slater determinant (e.g., $|\phi_0^2\phi_1^2\phi_3^2\rangle$ instead of $|\phi_0^2\phi_1^2\phi_2^2\rangle$ for a six-electron system). They are *impossible* to predict using the adiabatic approximation that is employed in all practical implementations of time-dependent DFT [22,23].

Figure 6 shows the low-lying singlet spectra of some selected molecules, computed using adiabatic TDLDA and eLDA. We choose glyoxal, benzoquinone, and tetrazine from the QuestDB dataset [89], as their low-lying spectra includes difficult-to-predict double excitations for which high-quality theoretical best estimate (TBE) results are available. They therefore serve as good examples to compare the eLDA approach with its TDLDA counterpart.

It is immediately clear that, for the lowest-lying excitations involving single promotion of an electron ("single excitations," single arrows in Fig. 6), eLDA predicts similar
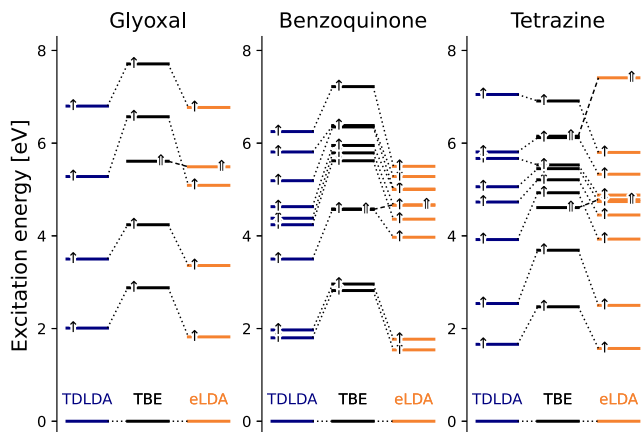

FIG. 6. Low-lying spectra (singlets only) of glyoxal, benzoquinone, and tetrazine predicted using TDLDA (navy) and eLDA (orange), compared against theoretical best estimate (TBE) values [89]. Connections between spectrum in approximations and TBE are shown using dotted lines, to facilitate comparisons. TDLDA captures single excitations (indicated by single arrows on the level line) but misses the double excitations (double arrows) entirely, so these connections are excluded from the plot.

excitation energies to TDLDA and thus has similar performance—albeit with a slight tendency to underestimate relative to TDLDA. However, unlike TDLDA, eLDA is also able to predict excitations involving *double* promotion of electrons ("double excitations," double arrows in Fig. 6) with a perfomance similar to that of single excitations. Thus, eLDA is nearly as good as TDLDA for low-lying excitations involving single promotion of an electron, but is also able to predict double promotions, unlike TDLDA. It therefore offers a major advance on TDLDA.

We also compute, but do not show, ΔSCF results for excited states, using the maximum overlap method (MOM) [90] to converge single and double promoted excited states within a self-consistent field framework based on LSDA. For the MOM calculations we employ the occupation factors from eLDA and promote only the ↑ electron in single excitations. We use PW92 correlation [10] as it is most similar to our cofe parametrization. Results for single excitations are almost identical to eLDA, with an overall mean absolute deviation of 1.08 eV from MOM compared to 1.05 eV for all single excitations shown in Fig. 6. However, double excitations are greatly improved by eLDA, with an mean absolute deviation of 0.67 eV using MOM being reduced to just 0.41 eV for eLDA. Again, we see that eLDA offers significant improvements.

Figure 6 also provides evidence that eLDA can be a cornerstone theory for better excited-state approximations, based on the following argument. As can be seen from the figure, TDLDA and eLDA yield very similar energies for most single excitations. The similarity of TDLDA and eLDA energies suggests that *all regular DFAs* are likely to yield similar energies for these excitations, whether evaluated as time-dependent DFAs or eDFAs—a theoretical justification for this argument is provided in Sec. III of Supplemental Material [79]. Thus, the 30 years of refinement of generalized gradient approximations (GGAs) and meta-GGAs (MGGAs) that has improved the quality of spectra predicted using TD(M)GGAs is likely to similarly improve spectra evaluated using e(M)GGAs. But e(M)GGAs may also exploit the extra degree of freedom enabled by the use of cofe gas physics and effective $\bar{f}(\boldsymbol{r})$.

In summary, we see that TDLDA fails quite dramatically for TS12 (Fig. 5 and related discussion) and cannot capture double excitations (Fig. 6), in contrast to an excellent (TS12) or impressive (double excitations) performance from eLDA on the difficult excitations. Errors in single excitation spectra (Fig. 6) from TDLDA and eLDA are similar. Directly, this shows that eLDA either improves excited-state predictions or does not make them worse. Indirectly, it has positive implications for refinements to eLDAs, e.g., eGGAs or eMGGAs.

VI. FUTURE PROSPECTS AND CONCLUSIONS

Ensemble density functional theory has recently benefited from a surge of fundamental understanding. This has

led to rapid advancements in extending, to excited states, the power of density functional theory for computing electronic structure of ground states. Especially, EDFT deals seamlessly with highly "quantum" states [44] (e.g., superpositions of Slater determinants and double excitations) of relevance to solar energy applications and quantum technologies.

However, despite an accumulation of successful applications, EDFT currently lacks a fully consistent framework for improving approximations, in the sense that it borrows density functional approximations which were originally designed for ground states as the key building blocks of the extended DFAs for excited states. In particular, computationally favorable modeling of singlet-singlet excitations does not include all the relevant correlations [27].

This work takes a first step toward deriving a novel family of DFAs specifically designed for excitations. It presents (Secs. III B and IV) the cornerstone models: the cofe homogeneous electron gas and the LDA for EDFT (eLDA). The cofe HEG is developed using an unnoticed— thus, so far, unexplored—class of nonthermal ensemble states of the HEG. Analytic expressions of the relevant (defined by two parameters, like LSDA) energy components are reported in Table I. Some of these components have no analogs in regular DFT but find home and use in EDFT. High- and low-density limits of the correlation energy have been found analytically.

The eLDA is derived by dividing the DFT energy expression into terms that need to be treated using the inhomogeneous system and those that are locally approximated using a cofe gas. Parametrizations for all terms required by the eLDA are derived and provided. An ansatz (consistent with one-electron, unpolarized, and cofe gas limits) is also made for the effective occupation factor of inhomogeneous systems, and is "normed" on doublet systems in lieu of semiclassical results.

The novel eLDA is then tested on a suite of important examples including ionization potentials, small triplet-singlet gaps, and low-lying excitations. These examples reveal that eLDA performs similarly to LSDA and/or TDLDA on problems where standard theories are known to work. However, it also performs very effectively on problems where LSDA and TDLDA fail—yielding excellent triplet-singlet gaps and impressive double excitation energies.

eLDA therefore readily offers an effective alternative to standard polarized-gas-based theories for both ground and excited-state problems. But we stress that its true potential lies as the cornerstone for *better* models and methodologies. What are the next natural steps to be considered? We finish with three suggestions.

  (i) It is vital to develop a generalized gradient approximation for cofe HEGs, to yield an eGGA along the lines of Eq. (45). The development of accurate GGAs

in the late 1980s and early 1990s greatly accelerated interest in DFT for ground states, by giving answers that were usefully predictive. eGGAs should do the same for excited states. Importantly, eGGAs would seamlessly integrate with existing hybrid-EDFT successes [43–45] and remove reliance on combination rules that (despite working unexpectedly well) are known to be incorrect for correlation [44]. From there, additional steps may readily be taken up an excited state Jacob's ladder [17], to gain systematic improvements in excited-state DFT modeling.

 (ii) The optimal way to model $\bar{f}(\boldsymbol{r})$ remains an open problem, and is entangled with (I) and semiclassical arguments. It would be useful to understand why Eq. (53) works so much better than Eq. (52) and how it can be improved. Exploiting exact relationships and useful norms is likely to lead to improved understanding and adaptation of $\bar{f}(\boldsymbol{r})$ in inhomogeneous systems, and thus improvements to the predictive ability of eLDA and any eDFAs built on it. Improved understanding of finite yet uniform electron gases may also help [66–69].

(iii) The cofe gas is not the only excited-state (ensemble) HEG that we could have used. As discussed in Sec. III B it is a logical and simple *two-parameter* model that yields appropriate limits yet incorporates excited-state physics in a way that is consistent with known conditions. But allowing for more parameters provides a wide scope for further generalizations and improvements. For example, in the spirit of Samal and Harbola [64], one might separate the density into core (density, n_{core}) orbitals that are all double occupied, and use a cofe-like treatment for the remaining orbitals—yielding a three-parameter HEG governed by n, n_{core}/n, and $\bar{f}$ that includes excited states.

The PYTHON code for studying and implementing the theory work in this paper is provided in Ref. [91,92]. The code to reproduce the atomic and molecular tests is available on request.

ACKNOWLEDGMENTS

APPENDIX A: EXCHANGE PROPERTIES OF cofe HEGs

Both ϵ_x and Π_x involve integrals of form

$$
\begin{aligned}
X_2[f] &:= \int_0^\infty \int_0^\infty f_{\max(q,q')} A(q,q') \frac{q'^2 dq'}{2\pi^2} \frac{q^2 dq}{2\pi^2} \\
&= 2 \int_0^\infty \int_{q'}^\infty f_q A(q,q') \frac{q^2 dq}{2\pi^2} \frac{q'^2 dq'}{2\pi^2} \\
&= 2 \int_0^\infty \int_0^\infty \Theta(q-q') f_q A(q,q') \frac{q'^2 dq'}{2\pi^2} \frac{q^2 dq}{2\pi^2} \\
&= \int_0^\infty f_q \bar{A}(q) \frac{q^2 dq}{2\pi^2},
\end{aligned}
\tag{A1}
$$

where $A(q,q') = A(q',q)$ and

$$
\bar{A}(q) = 2\int_0^q A(q,q') \frac{q'^2 dq'}{2\pi^2}.
$$

For ϵ_x we have $A(q,q') = V(q,q')$, where $\bar{V}(q) = 2\int_0^q V(q,q')(q'^2 dq'/2\pi^2) = (q/\pi)\int_0^1 \log(|1+x|/|1-x|)x\,dx = (q/\pi)$. We thus obtain Eq. (28) of the main text. To compute Π_x we can set $A(q,q') = 1$, where $\bar{1}(q) = 2\int_0^q (q'^2 dq'/2\pi^2) = (q^3/3\pi^2)$, and so we can easily compute Π_x given f_q. For cofe HEGs we obtain Eqs. (29) and (31).

The case of $n_{2,x}(R)$ is also covered by Eq. (A1), by setting $A(q,q';R) = \int e^{i(q-q')\cdot R}(d\hat{q}/4\pi)(d\hat{q}'/4\pi)$. However, this is rather painful to deal with in general. The special case of cofe HEGs is more easily handled by recognizing that $f_{\max(q,q')} = \bar{f}\Theta(\bar{k}_F - q)\Theta(\bar{k}_F - q')$. Then,

$$
n_{2,x}^{\text{cofe}}(R) = -\bar{f} \int_0^{\bar{k}_F} e^{iq\cdot R} \frac{dq}{(2\pi)^3} \int_0^{\bar{k}_F} e^{-iq'\cdot R} \frac{dq'}{(2\pi)^3}
\tag{A2}
$$

$$
= -\bar{f}\left| \frac{\bar{k}_F^3}{6\pi^2} g(\bar{k}_F R)\right|^2 \equiv -\Pi_x^{\text{cofe}} N(\bar{k}_F R),
\tag{A3}
$$

where $\Pi_x = -(n^2/\bar{f})$, $g(x) = 3[\sin(x) - x\cos(x)]/x^3$, and $N(x) = |g(x)|^2$. Thus, we obtain Eq. (30).

APPENDIX B: HARTREE PROPERTIES OF cofe HEGs

Let us consider Eqs. (19) and (20) for the special case of an HEG. First, we note that $n_{\kappa\kappa} = n$ for every state and, therefore, $n_{2,H} = n^2 + \Delta n_{2,H}$, where $\Delta n_{2,H}(r,r') = \sum_{\kappa \neq \kappa'} w_{\max(\kappa,\kappa')} n_{\kappa\kappa'}(r) n_{\kappa'\kappa}(r')$. Furthermore, the resulting pair density can depend only on $R = r - r'$ while symmetry means it depends only on $R = |r - r'|$. Thus,

$$
\Delta\epsilon_H = \frac{1}{N}\Delta E_H = \frac{1}{n}\int \Delta n_{2,H}(R) \frac{4\pi R^2 dR}{2R},
\tag{B1}
$$

where we used n^2 to cancel the background charge, $N = nV$ to cancel the integral over r, and symmetry to simplify the remaining integral over $r' = r + R$. Our goal is therefore to determine $\Delta n_{2,H}(R)$, Note that the working in this appendix is rather involved, so we will often drop superscripts w in working.

We are now ready to look at HEG ensembles. Consider a finite HEG of N electrons in a volume V, with density $n = N/V$. The orbitals are $\phi_q \approx (1/\sqrt{V})e^{iq\cdot r}$ for q on an appropriate reciprocal space grid. Each state $|\kappa\rangle$ has density $n_{s,\kappa\kappa}(r) = N/V = n$. The ground state is $|0\rangle = |q_1^2 \cdots q_{N/2}^2\rangle$ and is unpolarized. Other states may be described using $|\kappa\rangle = \hat{P}_{Q_\kappa}|0\rangle$, where $\hat{P}$ promotes Fock orbitals in the Slater determinant and $Q_\kappa := {}_{q_{i_1} \cdots q_{i_p}}^{q_{a_1} \cdots q_{a_p}}$ contains lists of from ($i \leq N/2$) and to ($a > N/2$) orbitals, including spin. Cross densities, when $\kappa \neq \kappa'$, are $n_{s,\kappa\kappa'}(r) = e^{i\Delta q_{\kappa\kappa'}\cdot r}/V$ or zero. The former result occurs if and only if Q_κ and $Q_{\kappa'}$ differ by a single orbital of the same spin, giving $\Delta q_{\kappa\kappa'} = q_{\in\kappa} - q_{\in\kappa'}$. We use "connected" (con) to refer to any pair of states κ and κ' that differ only by a single orbital, and call $\Delta q_{\kappa\kappa'}$ the connection wave number.

Let us now consider the case that N electrons are assigned to $N/2 \leq M \leq N$ orbitals, for a mean occupation of $f = (N/M)$. There are $\mathcal{N}_T = (2M)!/[(2M-N)!N!]$ total states once spin is accounted for, each of which is weighted by $w = (1/\mathcal{N}_T)$. Each of the $\mathcal{N}_T$ states $|\kappa\rangle$ has $N_{\uparrow,\downarrow,\kappa}$ electrons of each spin, giving $\zeta_\kappa = (N_{\uparrow,\kappa} - N_{\downarrow,\kappa})/N$. State $|\kappa\rangle$ is connected to C_κ other states. Since only one orbital may change at a time, we obtain $C_\kappa = N_{\uparrow,\kappa}(M - N_{\uparrow,\kappa}) + N_{\downarrow,\kappa}(M - N_{\downarrow,\kappa}) = NM - (N^2/2)(1 + \zeta_\kappa^2)$, where $N_{\uparrow,\downarrow,\kappa} \leq M$.

Our goal is to obtain useful properties of the Hartree pair density. The pair density is defined by

$$
\Delta n_{2,H}(R) = \frac{1}{\mathcal{N}_T} \sum_{\kappa,\kappa' \text{ con } \kappa} \frac{e^{i\Delta q_{\kappa\kappa'}\cdot R}}{V^2},
\tag{B2}
$$

where we used $w_\kappa = w_{\kappa'} = (1/\mathcal{N}_T)$ and $r - r' := R$. The special case of $r = r'$ ($R = 0$) yields the "on-top" pair density deviation, $\Pi_H = \Delta n_{2H}(R = 0)$, which is relatively straightforward to evaluate using $\Delta n_{2H} = (1/\mathcal{N}_T V^2)\sum_\kappa C_\kappa$, which follows from $e^{i\Delta q\cdot R} = 1$ for all connected states and the definition of C_κ. Using C_κ from the above paragraph yields

$$
\Delta\Pi_H = \frac{1}{V^2}\left[NM + \frac{N^2}{2}(1 + \bar{\zeta}^2)\right] = n^2\left[\frac{1}{f} - \frac{1 + \bar{\zeta}^2}{2}\right].
\tag{B3}
$$

where $\bar{\zeta}^2 = (1/\mathcal{N}_T)\sum_\kappa \zeta_\kappa^2$ is the ensemble averaged of the squared spin polarization.

As an initial test, consider the above analysis for the two special types of gases, unpolarized and fully polarized, which have no ensemble effects and which must therefore

yield $\Delta\Pi_H = 0$. An unpolarized gas involves $M = N/2$, $\bar{f} = 2$, $\mathcal{N}_T = 1$, and $\zeta_\kappa = 0$, yielding $\Delta\Pi_H = n^2(\frac{1}{2}-\frac{1}{2})=0$. A fully polarized gas involves $M = N$, $\bar{f} = 1$, $\mathcal{N}_T = 1$, and $\zeta_\kappa = 1$, yielding $\Delta\Pi_H = n^2(\frac{1}{1} - 1) = 0$. Thus, both exhibit the expected behavior. We therefore see that Eq. (B3) is consistent with existing results.

We are now ready to generalize to constant occupation factor ensemble (cofe) gases, with $f_q = \bar{f}\Theta(\bar{k}_F - q)$, for $1 < \bar{f} < 2$. As discussed in the main text, we restricted to the special case of maximally polarized states $|\kappa\rangle$, in which each state has the maximum spin polarization allowed by $\bar{f}$. All these states involve $N_\uparrow = M$ and $N_\downarrow = N - M$ giving $\zeta_\kappa = [(2M - N)/N] = (2/\bar{f}) - 1 = \bar{\zeta}$. Equation (B3) then yields

$$\Delta\Pi_H = n^2\frac{(2 - \bar{f})(\bar{f} - 1)}{\bar{f}^2}, \qquad \Pi_H = n^2\frac{3\bar{f} - 2}{\bar{f}^2}, \qquad \text{(B4)}$$

for the on-top, $\boldsymbol{R} = \boldsymbol{0}$, pair density.

We are now ready to move on from the on-top hole to consider general $\boldsymbol{R} \neq \boldsymbol{0}$. We first recognize that equal waiting of states is equivalent to equal weighting of connection wave numbers, yielding

$$\Delta n_{2,H}(\boldsymbol{R}) = \Delta\Pi_H\frac{1}{M^2}\sum_q\sum_{q'\neq q}e^{i(q-q')\cdot\boldsymbol{R}}$$
$$= \Delta\Pi_H\left[|g(\bar{k}_F R)|^2 - \frac{1}{M}\right], \qquad \text{(B5)}$$

where $g := (1/M)\sum_q e^{iq\cdot\boldsymbol{R}}$. We next impose symmetry on the wave numbers, and approximate the sum by an integral to obtain

$$g(\bar{k}_F R) \approx \frac{1}{M}\int_0^{(3M/4\pi)^{1/3}}\frac{\sin(qk_V R)}{qk_V R}4\pi q^2 dq$$
$$= \frac{3[\sin(\bar{k}_F R) - \bar{k}_F R\cos(\bar{k}_F R)]}{(\bar{k}_F R)^3}, \qquad \text{(B6)}$$

where $k_V = 2\pi/V^{1/3}$ is the wave number associated with the volume V, and $\bar{k}_F = (6\pi^2 M/V)^{1/3} = (6\pi^2 n/\bar{f})^{1/3}$ is the usual Fermi wave number. $g(x)$ is the same expression found in Eq. (A3). Note that $\Delta n_{2,H}(R)$ integrates to zero, as expected.

Finally, Eq. (B1) becomes $\Delta\epsilon_H = (\Delta\Pi_H/n) \times \{\int_0^\infty[g(\bar{k}_F R)^2/R]2\pi R^2 dR - (\bar{f}/2n)(9\pi/2V)^{1/3}\}$. In the limit $V \to \infty$ the second term vanishes, yielding

$$\Delta\epsilon_H^{\text{cofe}} = \bar{f}\Delta\Pi_H|\epsilon_x^{\text{cofe}}(r_s,\bar{f})| = \frac{C_H}{r_s}\frac{(2 - \bar{f})(\bar{f} - 1)}{\bar{f}^{4/3}} \qquad \text{(B7)}$$

$$= |\epsilon_x^{\text{cofe}}(r_s,\bar{f})|\frac{(2 - \bar{f})(\bar{f} - 1)}{\bar{f}}, \qquad \text{(B8)}$$

where we used $\epsilon_x^{\text{cofe}} = -(\bar{f}/n)\int_0^\infty\frac{g(\bar{k}_F R)^2}{R}2\pi R^2 dR$ [which follows from $n_{2,x}(R) = -\bar{f}g(\bar{k}_F R)^2$] and $\epsilon_x^{\text{cofe}} = (-C_x/r_s)[2/\bar{f}]^{1/3}$ derived in the main text, to obtain $C_H = 2^{1/3}C_x = 0.577252$. Similarly,

$$n_{2,H}(R) = n^2 + \Delta n_{2,H}(R) = n^2 + \Delta\Pi_H^{\text{cofe}}N(\bar{k}_F R), \qquad \text{(B9)}$$

where $\Delta\Pi_H^{\text{cofe}}$ is defined in Eq. (B4), and $N(x) = g(x)^2 = 9[\sin(x) - x\cos(x)]^2/x^6$ is the unitless function defined near Eq. (30) or Eq. (A3).

APPENDIX C: STATE-DRIVEN CORRELATION OF cofe HEGs

1. State-driven correlation energy from the random-phase approximation

The state-driven correlation energy [Eq. (41)] involves the response function at imaginary frequencies. The imaginary frequency density-density response of an unpolarized HEG is

$$\chi_0(q, i\omega; r_s) := -\frac{k_F}{4\pi^2}C\left(\frac{q}{2k_F}, \frac{\omega}{qk_F}\right), \qquad \text{(C1)}$$

where $k_F = 1.9191583/r_s = (3\pi^2 n)^{1/3}$ is the Fermi wave number of an unpolarized gas. Here,

$$C(Q,\Gamma) = 1 + \frac{\Gamma^2 - Q_+Q_-}{4Q}\log\frac{Q_+^2 + \Gamma^2}{Q_-^2 + \Gamma^2}$$
$$+ \Gamma\left[\tan^{-1}\frac{Q_-}{\Gamma} - \tan^{-1}\frac{Q_+}{\Gamma}\right], \qquad \text{(C2)}$$

where $Q_\pm = Q \pm 1$. For brevity we shall use $Q = (q/2k_F)$ and $\Gamma = (\omega/qk_F)$ to always mean unpolarized gas quantities.

For a polarized HEG we take half of two unpolarized systems with $k_{F\uparrow} = k_F(1 + \zeta)^{1/3} := k_Fh_+$ and $k_{F\downarrow} = k_F(1 - \zeta)^{1/3} := k_Fh_-$. Therefore,

$$\chi_0(q,\omega; r_s,\zeta) = -\frac{k_F}{8\pi^2}\left[h_+C\left(\frac{Q}{h_+},\frac{\Gamma}{h_+}\right) + h_-C\left(\frac{Q}{h_-},\frac{\Gamma}{h_-}\right)\right]. \qquad \text{(C3)}$$

The cofe case of constant $\bar{f}$ is easily dealt with by including a prefactor of $\bar{f}$ on χ_0 and using the cofe Fermi level, $\bar{k}_F = k_F(2/\bar{f})^{1/3} := k_Fg$. It follows from $\bar{f} = 2/g^3$ that

$$\chi_0^{\text{cofe}}(q,\omega; r_s,\bar{f}) = -\frac{k_F}{4\pi^2g^2}C\left(\frac{Q}{g},\frac{\Gamma}{g}\right). \qquad \text{(C4)}$$

Setting $\zeta = 0$ and $\bar{f} = 2$ yields $h_\pm = g = 1$ and yields the same response as the unpolarized gas. Similarly, setting

$\zeta = 1$ in Eq. (C3) gives the same result as setting $\bar{f} = 1$ in Eq. (C4), as expected.

From the response function we are able to evaluate the random-phase approximation for the correlation energy, via

$$\epsilon_c^{\mathrm{RPA}} = \frac{1}{2n} \int_0^\infty \frac{d\omega}{\pi} \int_0^\infty \frac{q^2 dq}{2\pi^2} \left[\chi_0 \frac{4\pi}{q^2} + \log\left(1 - \chi_0 \frac{4\pi}{q^2}\right) \right]. \tag{C5}$$

This may be made more convenient by using $n = (k_F^3/3\pi^2)$, $q = 2k_F Q$, and $\omega = q k_F \Gamma$ to write

$$\epsilon_c^{\mathrm{RPA}} = \frac{12 k_F^2}{\pi} I_{Q\Gamma}\left[\frac{\pi}{k_F^2 Q^2} \chi_0\right], \tag{C6}$$

where $I_{Q\Gamma}[f] := \int_0^\infty d\Gamma \int_0^\infty Q^3 dQ[-f + \log(1+f)]$. We may also define $\bar{I}(P) = I_{Q\Gamma}[(P/Q^2)C(Q,\Gamma)]$.

Thus, the RPA enhancement factor for a polarized gas, relative to an unpolarized gas at the same density, is

$$\xi_c^{\mathrm{RPA}}(\zeta) = \frac{I_{Q\Gamma}\left[\frac{Ph_+}{2Q^2}C(\frac{Q}{h_+}, \frac{\Gamma}{h_+}) + \frac{Ph_-}{2Q^2}C(\frac{Q}{h_-}, \frac{\Gamma}{h_-})\right]}{I_{Q\Gamma}\left[\frac{P}{Q^2}C(Q,\Gamma)\right]}$$
$$= \frac{h_+^5 \bar{I}(\frac{P}{2h_+}) + h_-^5 \bar{I}(\frac{P}{2h_-})}{\bar{I}(P)}, \tag{C7}$$

where $h_\pm = (1 \pm \zeta)^{1/3}$. The equivalent enhancement factor of a cof ensemble HEG may be written as

$$\xi_c^{\mathrm{RPA,cofe}}(\bar{f}) = \frac{I_{Q\Gamma}\left[\frac{P}{g^2 Q^2}C(\frac{Q}{g}, \frac{\Gamma}{g})\right]}{I_{Q\Gamma}\left[\frac{P}{Q^2}C(Q,\Gamma)\right]} = \frac{g^5 \bar{I}(\frac{P}{g^4})}{\bar{I}(P)}, \tag{C8}$$

where $P := (1/2\pi k_F) = 0.08293 r_s$ and $g = (2/\bar{f})^{1/3}$.

The RPA enhancement is expected to be accurate in the high-density of matter $k_F \to \infty$. Figure 7 shows (state-driven) correlation energy enhancement factors, $\xi_c^{\mathrm{RPA}}(\zeta)$ and $\xi_c^{\mathrm{RPA,cofe}}(f)$, as a function of the (average) occupation factor $\bar{f}$, using $\zeta = \hat{f}_{\mathrm{x\text{-}map}}^{-1}(\bar{f})$ [from Eq. (D8)] for the effective spin polarization. It reports ξ for high $(n = 10^6)$, medium $(n = 1)$, and low $(n = 10^{-6})$ densities. We see that the state-driven correlation energy of cofe HEGs is (i) virtually linear in $\bar{f}$, for high densities, and (ii) very similar to the (renormalized) on-top exchange enhancement factor, for low densities.

The high-density ($r_s \to 0$) behavior of ξ_c^{cofe} can be shown analytically, because $P \to 0$. We may therefore Taylor expand the log to obtain

$$\lim_{P\to\infty} \bar{I}(P) \approx \int_0^\infty Q^3 dQ \int_0^\infty d\Gamma \frac{1}{2}\left(\frac{P}{Q^2}C\right)^2, \tag{C9}$$

from which it follows that $\xi_c^{\mathrm{cofe}} = g^5 \bar{I}(P/g^4)/\bar{I}(P) = g^5(1/g^4)^2 = g^{-3} = \bar{f}/2$ is linear in $\bar{f}$. The RPA is not
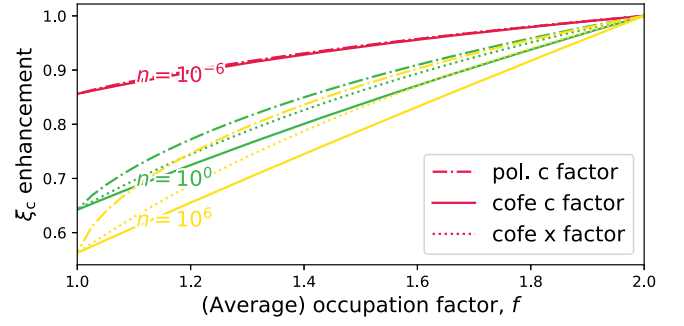

FIG. 7. Correlation enhancement of spin-polarized (dash-dotted lines) and cofe (solid lines) HEGs as a function of occupation factor f. The cofe exchange factor (dotted lines) is also shown after rescaling to yield the same vales for $\bar{f} = 1$ and $\bar{f} = 2$.

appropriate for the low-density limit, although we shall later see it is qualitatively correct.

2. State-driven correlation energies in general

We are now ready to use what we have learned about correlation energies from the RPA and theoretical arguments to obtain general expressions for the SD correlation energies in cofe HEGs. Let us begin with the low-density limit. The main text has shown that

$$\lim_{r_s\to\infty} \epsilon_c^{\mathrm{cofe}}(r_s, \bar{f}) = \epsilon_x(r_s)\left[\frac{C_\infty}{C_x} - f_{\mathrm{Hx}}^{\mathrm{cofe}}(\bar{f})\right]. \tag{C10}$$

It can also be shown that $\lim_{r_s\to\infty} \epsilon_c^{\mathrm{DD,cofe}}(r_s, \bar{f}) \to -\Delta\epsilon_{\mathrm{H}}^{\mathrm{cofe}}(r_s, \bar{f})$—this result is a specialized case of a broader relationship to be discussed in a future work. It is thus clear that the SD enhancement factor must capture the low-density scaling and cancel exchange:

$$\lim_{r_s\to\infty} \epsilon_c^{\mathrm{SD,cofe}}(r_s, \bar{f}) \to \epsilon_x(r_s)\left[\frac{C_\infty}{C_x} - f_x^{\mathrm{cofe}}(\bar{f})\right]. \tag{C11}$$

Surprisingly, this is consistent with the low-density behavior shown in Fig. 7 and so reveals that the RPA is qualitatively correct even in the low-density limit.

In the high-density limit, we instead obtain

$$\lim_{r_s\to 0} \epsilon_c^{\mathrm{SD,cofe}}(r_s, \bar{f}) \to (\bar{f} - 1)\epsilon_c^U + (2 - \bar{f})\epsilon_c^P$$
$$= \epsilon_c^U + (2 - \bar{f})[\epsilon_c^P - \epsilon_c^U], \tag{C12}$$

where $\epsilon_c^U := \epsilon_c(r_s, 0)$ is the correlation energy of an unpolarized gas, $\epsilon_c^P := \epsilon_c(r_s, 1)$ is the correlation energy of a fully polarized gas, and $2 - \bar{f} = [\xi^{\mathrm{RPA,cofe}}(\bar{f}) - \xi^{\mathrm{RPA}}(0)]/[\xi^{\mathrm{RPA}}(1) - \xi^{\mathrm{RPA}}(0)]$. This is analogous to the known result that

$$\lim_{r_s\to 0} \epsilon_c(r_s, \zeta) \to \epsilon_c^U + H^{\mathrm{RPA}}(\zeta)[\epsilon_c^P - \epsilon_c^U], \tag{C13}$$

where $H^{\text{RPA}}(\zeta) = -2[I(\zeta) - 1]$ is obtained from Eq. (32) of [93] or, equivalently, $H^{\text{RPA}}(\zeta) := [\xi^{\text{RPA}}(\zeta) - \xi^{\text{RPA}}(0)]/[\xi^{\text{RPA}}(1) - \xi^{\text{RPA}}(0)]$. We cannot say anything about the DD correlation energy in this limit.

We thus obtain limiting behaviors for high- and low-density HEGs. In typical polarized gases, one uses expansion in both limits together with QMC data, $\epsilon_c^{\text{QMC}}(r_s, \zeta)$, to fill in the gaps for moderate and large densities. We do not have QMC data for cofe gases. Thus, the final step in our analysis of correlation energies is to show how to reuse existing polarized gas QMC data for cofe HEGs.

As a first step, we assume that the high-density relationship [Eq. (C13)] between RPA and exact results is true for moderate and large r_s. That is, we expect

$$\bar{\xi}_c := 1 + \frac{\xi_c(\zeta = 1) - 1}{\xi_c^{\text{RPA}}(\zeta = 1) - 1}[\xi_c^{\text{RPA}} - 1] \approx \xi_c^{\text{QMC}} \qquad (\text{C14})$$

to be approximately valid for all r_s. The usefulness of this approximation is further supported by Fig. 7, which shows that the RPA yields an approximately linear dependence on $\bar{f}$ even for low-density HEGs where the RPA is expected to be poor.

The second step is to recognize that, in low-density gases, we may write $\xi_c = (C_\infty/C_x) - \xi_x$ and $\xi_c^{\text{SD,cofe}} = (C_\infty/C_x) + \xi_x^{\text{cofe}}$ and, therefore, $\epsilon_c^{\text{SD,cofe}}(r_s \to 0, \bar{f}) \approx X(\epsilon_x^{\text{cofe}}(r_s, \bar{f}))$, where $\epsilon_c(r_s \to 0, \zeta) := X(\epsilon_x(r_s, \zeta))$—here X is a single-variable function. Figure 8 shows that a similar result nearly holds for moderate r_s and, furthermore, that models of both cofe and polarized gases agree rather well with QMC data from Spink *et al.* [8], despite the data being for polarized gases. We therefore assume that

$$\epsilon_c^{\text{SD,cofe}}(r_s, \hat{f}_{\text{x-map}}(\zeta)) \approx \epsilon_c^{\text{QMC}}(r_s, \zeta) \qquad (\text{C15})$$

for moderate and large densities with viable QMC data, where $\hat{f}_{\text{x-map}}$ is defined such that $\epsilon_x(\zeta) = \epsilon_x^{\text{cofe}}(\bar{f} = \hat{f}_{\text{x-map}}(\zeta))$. This is a rather good approximation in practice as the maximum difference between $\epsilon_c^{\text{SD,cofe}}$ using RPA and $\epsilon_c^{\text{SD,cofe}}$ using Eq. (C15) is 1 mHa for $r_s = 1$, and is sub-mHa for larger r_s.

Thus, Eqs. (C12), (C15), and (C11) provide a set of constraints and reference values (from existing QMC data)
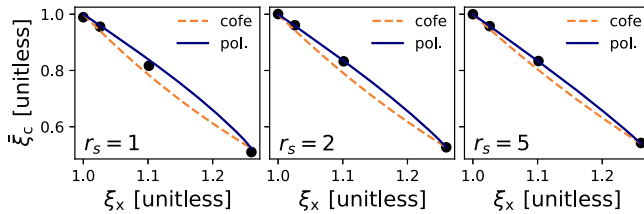

FIG. 8. $\bar{\xi}_c$ versus ξ_x using RPA data for cofe HEG (orange, dashed lines) and polarized HEG (navy, solid lines). Black dots indicate data from Ref. [8].

for high, moderate, and low densities, respectively. These three relationships are used in Appendix D to produce the parametrization for the state-driven correlation energy of a cofe HEG.

It would be very desirable to obtain QMC or similar-quality reference data for cofe HEGs, to provide direct inputs for parametrizations. The derivative, $de^{\text{cofe}}(r_s, \bar{f})/d\bar{f}|_{\bar{f}=2}$, may be amenable to computation using existing techniques, as it involves only low-lying excited states.

APPENDIX D: PARAMETRIZATIONS

The main text and previous appendixes have introduced five terms that go into the cofe HEG energy as a function of r_s and $\bar{f}$. This appendix will provide a useful parametrization of the state-driven correlation energy that will allow the use of cofe HEGs in density functional approximations. As explained in the main text, we propose

$$E_{\text{xc}}^{\text{eLDA}} := \int n(\mathbf{r})[\epsilon_x(r_s)f_x^{\text{cofe}}(\bar{f}) + \epsilon_c^{\text{SD,cofe}}(r_s, \bar{f})], \qquad (\text{D1})$$

where $r_s(\mathbf{r})$ and $\bar{f}(\mathbf{r})$ depend on local properties of the inhomogeneous system.

The exchange term involves the closed-form expression of Eq. (29). The correlation term, $\epsilon_c^{\text{SD,cofe}}(r_s, \bar{f})$, needs to be parametrized using the following.

(1) the known high-density behavior of Eq. (42),
(2) the known low-density behavior of Eq. (43),
(3) QMC data for other densities, adapted using Eq. (44).

The high-density limit yields [to $O[r_s \log(r_s)]$]

$$\epsilon_c^{\text{SD,cofe}}(r_s \to 0, \bar{f}) := c_0(\bar{f}) \log r_s - c_1(\bar{f}), \qquad (\text{D2})$$

where the parameters $c_{0,1}(\bar{f})$ are linear in $\bar{f}$ and are trivially related to their unpolarized and fully polarized counterparts [10]. The low-density limit yields [to $O(1/r_s^2)$]

$$\epsilon_c^{\text{SD,cofe}}(r_s \to \infty, \bar{f}) := \frac{-C_\infty + C_x[2/\bar{f}]^{1/3}}{r_s} + \frac{C_\infty'}{r_s^{3/2}}, \qquad (\text{D3})$$

where C_∞, C_x, and C_∞' are universal parameters that do not depend on $\bar{f}$ [50].

Perdew and Wang [10] proposed that HEG correlation energies lend themselves to a parametrization,

$$F(r_s; P) := -2A(1 + \alpha r_s) \log\left[1 + \frac{1}{2A\sum_{i=1}^4 \beta_i r_s^{i/2}}\right], \qquad (\text{D4})$$

where $P = (A, \alpha, \beta_1, \beta_2, \beta_3, \beta_4)$ is a set of parameters that depend on ζ, $\bar{f}$, or related variables. By construction, Eq. (D4) can be made exact to leading orders for small and large r_s. The high-density limit yields

$$A^{\mathrm{cofe}} = c_0, \qquad \beta_1^{\mathrm{cofe}} = \frac{e^{-c_1/(2c_0)}}{2c_0} \quad \beta_2^{\mathrm{cofe}} = 2A\beta_1^2, \qquad \text{(D5)}$$

where the coefficients are

$$c_0(\bar{f}) = \frac{0.031091\bar{f}}{2}, \qquad c_1(\bar{f}) = 0.00454 + \frac{0.0421\bar{f}}{2}.$$

The low-density limit yields

$$\beta_4^{\mathrm{cofe}} = \frac{\alpha}{C_\infty - C_x f_x^{\mathrm{cofe}}(\bar{f})}, \qquad \beta_3^{\mathrm{cofe}} = \frac{\beta_4^2 C'_\infty}{\alpha}, \qquad \text{(D6)}$$

using the parameters $C_\infty \approx 1.95C_x$ and $C'_\infty = 1.33$ [94] from Sec. III B 3 and $f_x^{\mathrm{cofe}}(\bar{f}) = [2/\bar{f}]^{1/3}$ from Eq. (29). Thus, only α is left undefined.

Our goal is to find parameters, $P(\bar{f})$, that can be used in a constant occupation factor parametrization, $\epsilon_c^{\mathrm{cofe}}(r_s, \bar{f}^*) :=$ $F[r_s; P^{\mathrm{cofe}}(\bar{f}^*)]$, of the cofe HEG at selected values of $\bar{f}^*$, and interpolated to general $\bar{f}$. Our first step is to pick the values of $\bar{f}^*$. We seek to adapt the high-quality QMC data of Spink *et al.* [8], who provided correlation energies for $\zeta^* \in (0, 0.34, 0.66, 1)$ using Eq. (44). We therefore seek parametrizations at $\bar{f}^* = \hat{f}_{\mathrm{x\text{-}map}}^{-1}(\zeta^*)$, so that the right-hand side of Eq. (44) is known.

As a first step, we must find $\hat{f}_{\mathrm{x\text{-}map}}$ and its inverse. Setting Eqs. (5) and (29) to be equal yields

$$\hat{f}_{\mathrm{x\text{-}map}}(\zeta) \approx 2 - \frac{4}{3}\zeta^2 + \frac{1}{6}[1.0187\zeta^3 + 0.9813\zeta^4], \qquad \text{(D7)}$$

$$\hat{f}_{\mathrm{x\text{-}map}}^{-1}(\bar{f}) \approx \sqrt{\frac{3}{4}(2-\bar{f})}\left[1 + \left(\sqrt{\frac{4}{3}} - 1\right)(2-\bar{f})\right], \qquad \text{(D8)}$$

which are exact in the polarized and unpolarized limits, and accurate to within 0.2% for all ζ and $\bar{f}$. Equation (D7) gives $\bar{f}^* \in (2, 1.85, 1.50, 1)$ for $\zeta^* \in (0, 0.34, 0.66, 1)$, which are the $\bar{f}$ values we use in fits. Then, for each $\bar{f}^*$, we obtain $\alpha(\bar{f}^*)$ by minimizing

$$\min_\alpha \sum_{r_s \in \mathrm{QMC}} |\epsilon_{c,\mathrm{QMC}}^{\zeta^{\mathrm{QMC}}}(r_s) - \epsilon_c^{\mathrm{SD,cofe}}(r_s, \bar{f}^*)|, \qquad \text{(D9)}$$

where $\epsilon_{c,\mathrm{QMC}}^{\zeta^{\mathrm{QMC}}}(r_s)$ is correlation energy data from Ref. [8] and $\epsilon_c^{\mathrm{SD,cofe}}(r_s, \bar{f}^*) := F(r_s, P(\bar{f}^*))$ involves the five constrained coefficients and free $\alpha(\bar{f}^*)$. Optimal parameters for the four values of ζ^* (called ζ^{QMC} to highlight their origin) are reported in Table II.

The next step of our parametrization departs from PW92, in that we approximate the correlation energy at arbitrary $\bar{f}$ via cubic fits (in $\bar{f}$) to the QMC data. Thus,

$$\epsilon_c^{\mathrm{cofe}}(r_s, \bar{f}) := (\bar{f}-1)\epsilon_c^0(r_s) + (2-\bar{f})\epsilon_c^1(r_s)$$
$$+ (\bar{f}-1)(2-\bar{f})\left[M_2(r_s) + \left(\frac{3}{2} - \bar{f}\right)M_3(r_s)\right], \tag{D10}$$

where $\epsilon_c^\zeta(r_s) := F(r_s, P_\zeta)$ is computed using Eq. (D4) and M_2 and M_3 involve weighted sums of $\epsilon_c(r_s, \bar{f})$ at selected values of $\bar{f}$. This fit becomes exact in the high-density limit, as the correlation energy is linear in $\bar{f}$, and is also extremely accurate in the low-density limit as $(2/\bar{f})^{1/3}$ for $\bar{f} \in [1, 2]$ may be reproduced to within 0.1% by a cubic fit. A cubic fit on $\bar{f}^* \in (2, 1.85, 1.50, 1)$ yields

$$M_2(r_s) := 2[2\epsilon_c^{0.66}(r_s) - \epsilon_c^0(r_s) - \epsilon_c^1(r_s)], \tag{D11}$$

$$M_3(r_s) := \frac{40}{357}[102\epsilon_c^{0.66}(r_s) - 200\epsilon_c^{0.34}(r_s)$$
$$+ 119\epsilon_c^1(r_s) - 21\epsilon_c^0(r_s)], \tag{D12}$$

where α is optimized on each of the four spin polarizations.

The same strategy may also be applied to a conventional spin-polarized HEG. Thus, in addition to parameters for the cofe model, Tables II and III also contain a set of coefficients for a "revised PW92" (rPW92) model that is an analog of the cofe model introduced here. Details are provided in Appendix E. As it is based on similar principles, rPW92 is more directly comparable to the cofe parametrization provided here than the original PW92, especially in the low-density limit.
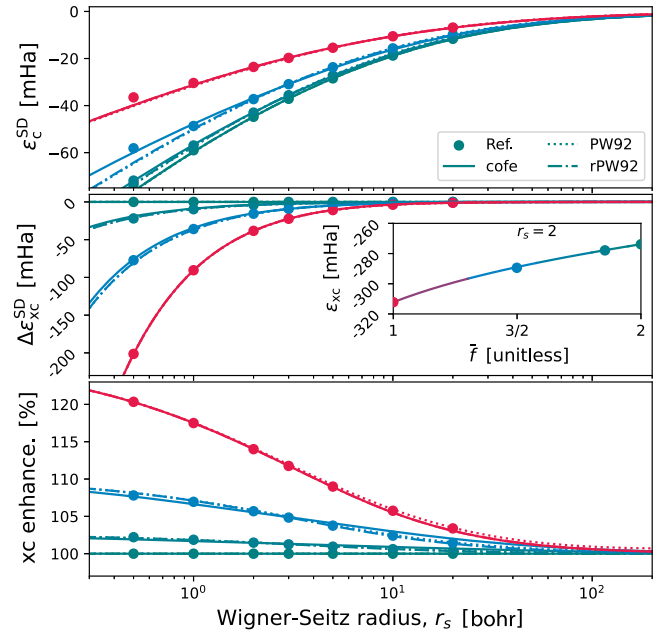

FIG. 9. Like Fig. 3 but with the addition of polarized HEG results from PW92 [10] (dots) and rPW92 (dash-dotted line) for $\zeta \in (0, 0.34, 0.66, 1)$, to show differences between cofe and polarized gases in the high-density limit.

APPENDIX E: REVISED PW92

The revised PW92 parametrization is designed as a direct replacement for the original PW92 model [10]. Its main differences are (1) the use of a cubic fit in ζ^2, analogous to the fit to $\bar{f}$ used in the main text, (2) the use of the most up-to-date understanding of the low-density limit, per Sec. III B 3, and (3) α is found from the Spink reference data [8]. Note that we fit to ζ^2 because exchange and correlation are quadratic for $\zeta \to 0$, but linear for $\bar{f} \to 2$.

The rPW92 parametrization of correlation energies is

$$\epsilon_c^{\mathrm{rPW92}}(r_s, \zeta) := (1 - \zeta^2)\epsilon_c^0 + \zeta^2 \epsilon_c^1$$
$$+ (1 - \zeta^2)\zeta^2[Z_2(r_s) + \zeta^2 Z_3(r_s)], \quad \text{(E1)}$$

where coefficients for $Z_{2,3}$ are reported in Table III. Interestingly, the values we obtain for α at $\zeta = 0$ and $\zeta = 1$ are slightly lower than those from the original PW92 parametrization [10], most likely due to the use of more modern QMC data.

Figure 9 shows results from Fig. 3 plus the LSDA (rPW92) parametrized along similar lines. It also includes results from an existing LSDA (PW92 [10]). By construction, both cofe and rPW92 do a better job of capturing the strictly correlated electron limit, especially as PW92 incorrectly yields different low-density behaviors for different ζ. It is important to recognize that differences (for $\zeta = 0.34$ and 0.66) between cofe enhancement factors and PW92 and rPW92 do not represent errors, but rather represent different quantum physics captured by cofe and polarized gases, which lead to different high-density behaviors.

---

[1] P. Hohenberg and W. Kohn, *Inhomogeneous electron gas*, Phys. Rev. **136**, B864 (1964).

[2] W. Kohn and L. J. Sham, *Self-consistent equations including exchange and correlation effects*, Phys. Rev. **140**, A1133 (1965).

[3] L. H. Thomas, *The calculation of atomic fields*, Math. Proc. Cambridge Philos. Soc. **23**, 542 (1927).

[4] E. Fermi, *Un metodo statistico per la determinazione di alcune proprieta dell'atomo*, Rend. Accad. Naz. Lincei **6**, 602 (1927).

[5] Also known as jellium or uniform electron gas—we use HEG exclusively throughout.

[6] D. M. Ceperley and B. J. Alder, *Ground state of the electron gas by a stochastic method*, Phys. Rev. Lett. **45**, 566 (1980).

[7] F. H. Zong, C. Lin, and D. M. Ceperley, *Spin polarization of the low-density three-dimensional electron gas*, Phys. Rev. E **66**, 036703 (2002).

[8] G. G. Spink, R. J. Needs, and N. D. Drummond, *Quantum Monte Carlo study of the three-dimensional spin-polarized homogeneous electron gas*, Phys. Rev. B **88**, 085121 (2013).

[9] S. H. Vosko, L. Wilk, and M. Nusair, *Accurate spin-dependent electron liquid correlation energies for local spin density calculations: A critical analysis*, Can. J. Phys. **58**, 1200 (1980).

[10] J. P. Perdew and Y. Wang, *Accurate and simple analytic representation of the electron-gas correlation energy*, Phys. Rev. B **45**, 13244 (1992).

[11] T. Chachiyo, *Communication: Simple and accurate uniform electron gas correlation energy for the full range of densities*, J. Chem. Phys. **145**, 021101 (2016).

[12] E. H. Lieb and B. Simon, *Thomas-Fermi theory revisited*, Phys. Rev. Lett. **31**, 681 (1973).

[13] E. H. Lieb and B. Simon, *The Thomas-Fermi theory of atoms, molecules and solids*, Adv. Math. **23**, 22 (1977).

[14] E. H. Lieb, *Thomas-Fermi and related theories of atoms and molecules*, Rev. Mod. Phys. **53**, 603 (1981).

[15] P. Elliott, D. Lee, A. Cangi, and K. Burke, *Semiclassical origins of density functionals*, Phys. Rev. Lett. **100**, 256406 (2008).

[16] K. Burke, A. Cancio, T. Gould, and S. Pittalis, *Locality of correlation in density functional theory*, J. Chem. Phys. **145**, 054112 (2016).

[17] J. P. Perdew and K. Schmidt, *Jacob's ladder of density functional approximations for the exchange-correlation energy*, AIP Conf. Proc. **577**, 1 (2001).

[18] A. D. Becke, *Density-functional exchange-energy approximation with correct asymptotic behavior*, Phys. Rev. A **38**, 3098 (1988).

[19] J. P. Perdew, K. Burke, and M. Ernzerhof, *Generalized gradient approximation made simple*, Phys. Rev. Lett. **77**, 3865 (1996).

[20] J. Sun, A. Ruzsinszky, and J. P. Perdew, *Strongly constrained and appropriately normed semilocal density functional*, Phys. Rev. Lett. **115**, 036402 (2015).

[21] J.-D. Chai and M. Head-Gordon, *Systematic optimization of long-range corrected hybrid density functionals*, J. Chem. Phys. **128**, 084106 (2008).

[22] N. T. Maitra, F. Zhang, R. J. Cave, and K. Burke, *Double excitations within time-dependent density functional theory linear response*, J. Chem. Phys. **120**, 5932 (2004).

[23] N. T. Maitra, *Undoing static correlation: Long-range charge transfer in time-dependent density-functional theory*, J. Chem. Phys. **122**, 234104 (2005).

[24] H. Iikura, T. Tsuneda, T. Yanai, and K. Hirao, *A long-range correction scheme for generalized-gradient-approximation exchange functionals*, J. Chem. Phys. **115**, 3540 (2001).

[25] T. Stein, L. Kronik, and R. Baer, *Reliable prediction of charge transfer excitations in molecular complexes using time-dependent density functional theory*, J. Am. Chem. Soc. **131**, 2818 (2009).

[26] N. T. Maitra, *Charge transfer in time-dependent density functional theory*, J. Phys. Condens. Matter **29**, 423001 (2017).

[27] P. de Silva, *Inverted singlet-triplet gaps and their relevance to thermally activated delayed fluorescence*, J. Phys. Chem. Lett. **10**, 5674 (2019).

[28] J. Ehrmaier, E. J. Rabe, S. R. Pristash, K. L. Corp, C. W. Schlenker, A. L. Sobolewski, and W. Domcke, *Singlet-triplet inversion in heptazine and in polymeric carbon nitrides*, J. Phys. Chem. A **123**, 8099 (2019).

[29] S. Ghosh and K. Bhattacharyya, *Origin of the failure of density functional theories in predicting inverted singlet-triplet gaps*, J. Phys. Chem. A **126**, 1378 (2022).

[30] E. K. U. Gross, L. N. Oliveira, and W. Kohn, *Rayleigh-Ritz variational principle for ensembles of fractionally occupied states*, Phys. Rev. A **37,** 2805 (1988).

[31] E. K. U. Gross, L. N. Oliveira, and W. Kohn, *Density-functional theory for ensembles of fractionally occupied states. I. Basic formalism*, Phys. Rev. A **37,** 2809 (1988).

[32] E. Pastorczak and K. Pernal, *Ensemble density variational methods with self- and ghost-interaction-corrected functionals*, J. Chem. Phys. **140,** 18A514 (2014).

[33] M. Filatov, M. Huix-Rotllant, and I. Burghardt, *Ensemble density functional theory method correctly describes bond dissociation, excited state electron transfer, and double excitations*, J. Chem. Phys. **142,** 184104 (2015).

[34] M. Filatov, *Ensemble DFT approach to excited states of strongly correlated molecular systems*, in *Density-Functional Methods for Excited States*, edited by N. Ferré, M. Filatov, and M. Huix-Rotllant (Springer International Publishing, Cham, 2016), pp. 97–124.

[35] A. Pribram-Jones, Z.-h. Yang, J. R. Trail, K. Burke, R. J. Needs, and C. A. Ullrich, *Excitations and benchmark ensemble density functional theory for two electrons*, J. Chem. Phys. **140,** 18A541 (2014).

[36] Z.-H. Yang, J. R. Trail, A. Pribram-Jones, K. Burke, R. J. Needs, and C. A. Ullrich, *Exact and approximate Kohn-Sham potentials in ensemble density-functional theory*, Phys. Rev. A **90,** 042501 (2014).

[37] Z.-H. Yang, A. Pribram-Jones, K. Burke, and C. A. Ullrich, *Direct extraction of excitation energies from ensemble density-functional theory*, Phys. Rev. Lett. **119,** 033003 (2017).

[38] T. Gould, L. Kronik, and S. Pittalis, *Charge transfer excitations from exact and approximate ensemble Kohn-Sham theory*, J. Chem. Phys. **148,** 174101 (2018).

[39] F. Sagredo and K. Burke, *Accurate double excitations from ensemble density functional calculations*, J. Chem. Phys. **149,** 134103 (2018).

[40] K. Deur and E. Fromager, *Ground and excited energy levels can be extracted exactly from a single ensemble density-functional theory calculation*, J. Chem. Phys. **150,** 094106 (2019).

[41] P.-F. Loos and E. Fromager, *A weight-dependent local correlation density-functional approximation for ensembles*, J. Chem. Phys., **152,** 214101 (2020).

[42] C. Marut, B. Senjean, E. Fromager, and P.-F. Loos, *Weight dependence of local exchange-correlation functionals in ensemble density-functional theory: Double excitations in two-electron systems*, Faraday Discuss. **224,** 402 (2020).

[43] T. Gould, *Approximately self-consistent ensemble density functional theory with all correlations*, J. Phys. Chem. Lett. **11,** 9907 (2020).

[44] T. Gould, L. Kronik, and S. Pittalis, *Double excitations in molecules from ensemble density functionals: Theory and approximations*, Phys. Rev. A **104,** 022803 (2021).

[45] T. Gould, Z. Hashimi, L. Kronik, and S. G. Dale, *Single excitation energies obtained from the ensemble "HOMO–LUMO gap": Exact results and approximations*, J. Phys. Chem. Lett. **13,** 2452 (2022).

[46] T. Gould and S. Pittalis, *Hartree and exchange in ensemble density functional theory: Avoiding the nonuniqueness disaster*, Phys. Rev. Lett. **119,** 243001 (2017).

[47] T. Gould and S. Pittalis, *Density-driven correlations in many-electron ensembles: Theory and application for excited states*, Phys. Rev. Lett. **123,** 016401 (2019).

[48] E. Fromager, *Individual correlations in ensemble density-functional theory: State-driven/density-driven decompositions without additional Kohn-Sham systems*, Phys. Rev. Lett. **124,** 243001 (2020).

[49] T. Gould, G. Stefanucci, and S. Pittalis, *Ensemble density functional theory: Insight from the fluctuation-dissipation theorem*, Phys. Rev. Lett. **125,** 233001 (2020).

[50] T. Gould, D. P. Kooi, P. Gori-Giorgi, and S. Pittalis, *Electronic excited states in extreme limits via ensemble density functionals*, Phys. Rev. Lett. **130,** 106401 (2023).

[51] J. Kirkpatrick, B. McMorrow, D. H. P. Turban, A. L. Gaunt, J. S. Spencer, A. G. D. G. Matthews, A. Obika, L. Thiry, M. Fortunato, D. Pfau, L. R. Castellanos, S. Petersen, A. W. R. Nelson, P. Kohli, P. Mori-Sánchez, D. Hassabis, and A. J. Cohen, *Pushing the frontiers of density functionals by solving the fractional electron problem*, Science **374,** 1385 (2021).

[52] M. Levy, *Universal variational functionals of electron densities, first-order density matrices, and natural spin-orbitals and solution of the v-representability problem*, Proc. Natl. Acad. Sci. U.S.A. **76,** 6062 (1979).

[53] E. H. Lieb, *Density functionals for Coulomb systems*, Int. J. Quantum Chem. **24,** 243 (1983).

[54] U. von Barth and L. Hedin, *A local exchange-correlation potential for the spin polarized case. I*, J. Phys. C **5,** 1629 (1972).

[55] Note that here we mean "exact" in the sense that of the exact form, not the functional obtained at the exact density and orbitals.

[56] A. Pribram-Jones, D. A. Gross, and K. Burke, *DFT: A theory full of holes?*, Annu. Rev. Phys. Chem. **66,** 283 (2015).

[57] E. H. Lieb and S. Oxford, *Improved lower bound on the indirect Coulomb energy*, Int. J. Quantum Chem. **19,** 427 (1981).

[58] O. Gunnarsson and B. I. Lundqvist, *Exchange and correlation in atoms, molecules, and solids by the spin-density-functional formalism*, Phys. Rev. B **13,** 4274 (1976).

[59] C.-L. Cheng, Q. Wu, and T. Van Voorhis, *Rydberg energies using excited state density functional theory*, J. Chem. Phys. **129,** 124112 (2008).

[60] G. Levi, A. V. Ivanov, and H. Jónsson, *Variational density functional calculations of excited states via direct optimization*, J. Chem. Theory Comput. **16,** 6968 (2020).

[61] W. Kohn, *Density-functional theory for excited states in a quasi-local-density approximation*, Phys. Rev. A **34,** 737 (1986).

[62] L. N. Oliveira, E. K. U. Gross, and W. Kohn, *Density-functional theory for ensembles of fractionally occupied states. II. Application to the He atom*, Phys. Rev. A **37,** 2821 (1988).

[63] A. K. Theophilou and P. G. Papaconstantinou, *Local spin-density approximation for spin eigenspaces and its application to the excited states of atoms*, Phys. Rev. A **61,** 022502 (2000).

[64] P. Samal and M. K. Harbola, *Local-density approximation for the exchange energy functional in excited-state density functional theory*, J. Phys. B **38,** 3765 (2005).

[65] M. Hemanadhan, M. Shamim, and M. K. Harbola, *Testing an excited-state energy density functional and the associated potential with the ionization potential theorem*, J. Phys. B **47**, 115005 (2014).

[66] P.-F. Loos and P. M. W. Gill, *Exact wave functions of two-electron quantum rings*, Phys. Rev. Lett. **108**, 083002 (2012).

[67] P.-F. Loos and P. M. W. Gill, *Uniform electron gases. I. Electrons on a ring*, J. Chem. Phys. **138**, 164124 (2013).

[68] P.-F. Loos, C. J. Ball, and P. M. W. Gill, *Uniform electron gases. II. The generalized local density approximation in one dimension*, J. Chem. Phys. **140**, 18A524 (2014).

[69] P.-F. Loos, *Generalized local-density approximation and one-dimensional finite uniform electron gases*, Phys. Rev. A **89**, 052523 (2014).

[70] J. P. Perdew, R. G. Parr, M. Levy, and J. L. Balduz, *Density-functional theory for fractional particle number: Derivative discontinuities of the energy*, Phys. Rev. Lett. **49**, 1691 (1982).

[71] "'cofe' is pronounced like coffee by the authors.

[72] E. Wigner, *On the interaction of electrons in metals*, Phys. Rev. **46**, 1002 (1934).

[73] E. Wigner, *Effects of the electron interaction on the energy levels of electrons in metals*, Trans. Faraday Soc. **34**, 678 (1938).

[74] S. Azadi and N. D. Drummond, *Low-density phase diagram of the three-dimensional electron gas*, Phys. Rev. B **105**, 245135 (2022).

[75] E. Alves, G. L. Bendazzoli, S. Evangelisti, and J. A. Berger, *Accurate ground-state energies of Wigner crystals from a simple real-space approach*, Phys. Rev. B **103**, 245125 (2021).

[76] S. Śmiga, F. D. Sala, P. Gori-Giorgi, and E. Fabiano, *Self-consistent implementation of Kohn–Sham adiabatic connection models with improved treatment of the strong-interaction limit*, J. Chem. Theory Comput. **18**, 5936 (2022).

[77] Or level specific contributions, in case of degeneracies. To keep notation and illustrations simple, as done also before, we shall not explicate all the details.

[78] T. Gould, *Stationary conditions for excited states: The surprising impact of density-driven correlations*, arXiv: 2404.12593.

[79] See Supplemental Material at http://link.aps.org/supplemental/10.1103/PhysRevX.14.041045 for (i) additional theory about effective occupation factors; (ii) additional theory and technical details about the calculations; and (iii) Additional theoretical analysis of similarities in TDLDA and eLDA, which includes Ref. [80].

[80] G. Levi, A. V. Ivanov, and H. Jónsson, *Variational calculations of excited states via direct optimization of the orbitals in DFT*, Faraday Discuss. **224**, 448 (2020).

[81] This relationship follows from the fluctuation-dissipation theory for DFT, as it relates xc pair densities (and thus xc holes) to frequency integrals over density-density response functions [49].

[82] R. M. Parrish, L. A. Burns, D. G. A. Smith, A. C. Simmonett, A. E. DePrince, E. G. Hohenstein, U. Bozkaya, A. Y. Sokolov, R. D. Remigio, R. M. Richard *et al.*, PSI4 1.1: *An open-source electronic structure program emphasizing automation, advanced libraries, and interoperability*, J. Chem. Theory Comput. **13**, 3185 (2017).

[83] D. G. A. Smith, L. A. Burns, D. A. Sirianni, D. R. Nascimento, A. Kumar, A. M. James, J. B. Schriber, T. Zhang, B. Zhang, A. S. Abbott *et al.*, PSI4NUMPY: *An interactive quantum chemistry programming environment for reference implementations and rapid development*, J. Chem. Theory Comput. **14**, 3504 (2018).

[84] Q. Sun, T. C. Berkelbach, N. S. Blunt, G. H. Booth, S. Guo, Z. Li, J. Liu, J. D. McClain, E. R. Sayfutyarova, S. Sharma, S. Wouters, and G. K.-L. Chan, PYSCF: *The PYTHON-based simulations of chemistry framework*, WIREs Comput. Mol. Sci. **8**, e1340 (2017).

[85] Q. Sun, X. Zhang, S. Banerjee, P. Bao, M. Barbry, N. S. Blunt, N. A. Bogdanov, G. H. Booth, J. Chen, Z.-H. Cui *et al.*, *Recent developments in the PYSCF program package*, J. Chem. Phys. **153**, 024109 (2020).

[86] J. Lee and M. Head-Gordon, *Two single-reference approaches to singlet biradicaloid problems: Complex, restricted orbitals and approximate spin-projection combined with regularized orbital-optimized Møller-Plesset perturbation theory*, J. Chem. Phys. **150**, 244106 (2019).

[87] J. Lee, L. W. Bertels, D. W. Small, and M. Head-Gordon, *Kohn-Sham density functional theory with complex, spin-restricted orbitals: Accessing a new class of densities without the symmetry dilemma*, Phys. Rev. Lett. **123**, 113001 (2019).

[88] J. P. Perdew, A. Ruzsinszky, J. Sun, N. K. Nepal, and A. D. Kaplan, *Interpretations of ground-state symmetry breaking and strong correlation in wavefunction and density functional theories*, Proc. Natl. Acad. Sci. U.S.A. **118**, e2017850118 (2021).

[89] M. Véril, A. Scemama, M. Caffarel, F. Lipparini, M. Boggio-Pasqua, D. Jacquemin, and P.-F. Loos, QUESTDB: *A database of highly accurate excitation energies for the electronic structure community*, WIREs Comput. Mol. Sci. **11**, e1517 (2021).

[90] A. T. B. Gilbert, N. A. Besley, and P. M. W. Gill, *Self-consistent field calculations of excited states using the maximum overlap method (MOM)*, J. Phys. Chem. A **112**, 13164 (2008).

[91] https://github.com/gambort/cofHEG.

[92] T. Gould, *Supporting code and data for the paper "Local Density Approximation for Excited State"*, Zenodo (2024), 10.5281/zenodo.13927864.

[93] Y. Wang and J. P. Perdew, *Correlation hole of the spin-polarized electron gas, with exact small-wave-vector and high-density scaling*, Phys. Rev. B **44**, 13298 (1991).

[94] M. Seidl, S. Giarrusso, S. Vuckovic, E. Fabiano, and P. Gori-Giorgi, *Communication: Strong-interaction limit of an adiabatic connection in Hartree-Fock theory*, J. Chem. Phys. **149**, 241101 (2018).